Sequence-function Relationships in Phage-encoded Bacterial Cell Wall Lytic Enzymes and their Implications for Phage-derived Products Design

Roberto Vázquez,[a,b]* Ernesto García,[a,b] Pedro García[a,b]

RV: https://orcid.org/0000-0002-7919-552X

EG: https://orcid.org/0000-0002-1741-5486

PG: https://orcid.org/0000-0001-6717-8717

[a]Departamento de Biotecnología Microbiana y de Plantas, Centro de Investigaciones Biológicas Margarita Salas (CIB-CSIC), Madrid, Spain

[b]Centro de Investigación Biomédica en Red de Enfermedades Respiratorias (CIBERES), Madrid, Spain

*Address correspondence to Roberto Vázquez, rvazquez@cib.csic.es

Running title: Bioinformatic analysis of phage lysin sequences

Abstract: 375 words (Abstract: 227 words; Importance: 148 words)

Main text: 6172 words

ABSTRACT Phage (endo)lysins are thought to be a viable alternative to usual antibiotic chemotherapy to fight resistant bacterial infections. However, a landscape view of lysins' structure and properties regarding their function, with an applied focus, is somewhat lacking. Current literature suggests that specific features typical of lysins from phages infecting Gram-negative bacteria (G−) (higher net charge, amphipathic helices) are responsible for an improved interaction with G− envelope. Such antimicrobial peptide (AMP)-like elements are also of interest for antimicrobial molecules design. Thus, this study aims to provide an updated view on the primary structural landscape of phage lysins to clarify the evolutionary importance of several sequence-predicted properties, particularly for the interaction with the G− surface. A database of 2,182 lysin sequences was compiled, containing relevant information such as domain architectures, data on the phages' host bacteria and sequence-predicted physicochemical properties. Based on such classifiers, an investigation on the differential appearance of certain features was conducted. Such analyses revealed different lysin architectural variants that are preferably found in phages infecting certain bacterial hosts. Particularly, some physicochemical properties (higher net charge, hydrophobicity, hydrophobic moment and aliphatic index) were associated to G− phage lysins, appearing specifically at their C-terminal end. Evidences on the remarkable genetic specialization of lysins regarding the features of the bacterial hosts have been provided, specifically supporting the nowadays common hypothesis that lysins from G− usually contain AMP-like regions.

IMPORTANCE Phage-encoded lytic enzymes, also called lysins, are one of the most promising alternatives to common antibiotics. The lysins potential as novel antimicrobials to tackle antibiotic-resistant bacteria not only arises from features such as a lower chance to provoke resistance, but also from their versatility as synthetic biology

parts. Functional modules derived from lysins are currently being used for the design of novel antimicrobials with desired properties. This study provides a view of the lysins diversity landscape by examining a set of phage lysin genes. This way, we have uncovered the fundamental differences between the lysins from phages that infect bacteria with different superficial architectures, and, thus, also the reach of their specialization regarding cell wall structures. These results provide clarity and evidences to sustain some of the common hypothesis in current literature, as well as make available an updated and characterized database of lysins sequences for further developments.

KEYWORDS endolysins, bacteriophages, bacteriophage therapy, genomics, bioinformatics, antimicrobial agents

INTRODUCTION

Since the antibiotic pipeline started drying out, a worrying increase in the antibiotic resistant fraction of bacterial populations has been reported (1, 2), and highly antibiotic-resistant population percentages have maintained (3, 4). Thus, if the situation is set to continue, the cost, both economic and in human lives, will be enormous due to the lack of effective treatments (5, 6). This has prompted the interest in novel antimicrobials development by many public health actors, such as international overseeing organizations (7), public health and disease control agencies (3, 4), governments (8), researchers, and several companies (9). Some of the current efforts to gather a new antimicrobial armamentarium have led science towards bacteriophages (phages) (10, 11).

To allow the dissemination of the progeny, double-stranded DNA phages provoke the bacterial host lysis, which is fundamentally accomplished by degradation of the peptidoglycan. This polymer is an essential constituent of the bacterial cell wall, and the breakage of specific bonds within its three-dimensional mesh leads to bacterial death, largely by osmotic shock. The main phage molecule responsible for peptidoglycan degradation is the lysin (also referred to as endolysin). Lysins are released towards their polymeric target, usually with the assistance of another kind of proteins, the holins, which create pores in the plasma membrane and thus allow lysins leakage to the periplasm (12). There are also other phage products that collaborate in hampering the cell wall in some of its particular settings; for example, lysins B detach the arabino-mycolyl outer layer of mycobacteria and their relatives (*e.g.*, *Rhodococcus*, *Corynebacterium*) (13). Besides, in some Gram-negative bacteria (G–), effective lysis also needs the concurrence of additional phage products named spanins (14). This reveals the important amount of genetic resources put up by phages to overcome the barriers that the bacterial cell walls represent.

In addition to using whole phage particles as therapeutic agents against bacterial infections (the so-called ‘phage therapy’), current efforts also point out to artificially repurposing certain phage products, such as lysins, as antimicrobials (‘enzybiotics’) themselves (11, 15, 16). The concept is rather simple: the external addition of purified lysins to a susceptible bacterium would cause bacterial lysis whenever the lysin degrades the peptidoglycan. This process has been shown to be straightforward in the case of Gram-positive bacteria (G+) and the therapeutic effect of enzybiotics on G+ has been fully confirmed experimentally (15). The most important characteristics that make enzybiotics amenable to be postulated as therapeutics are: a) a certain specificity towards the original bacterial host and some closely related bacteria, that would prevent

93 normal microbiota to be harmed (16, 17), or, conversely, the possibility to have broad-
94 range lysins, if needed (18); b) a lower chance to provoke the appearance of resistant
95 bacteria, which is speculated to be because of the essential nature of the highly
96 conserved peptidoglycan (this is, changes in its structure lead to a decreased fitness
97 and/or virulence) (19); c) neither adverse immune responses nor production of
98 neutralizing antibodies are expected, possibly due to the usual presence of phages —and
99 their products— among the normal cohabitating microbial populations in humans (20).
100 Moreover, lysins are amenable for protein engineering strategies (18, 21–24). Typically,
101 the architectural organization of lysins comprises one (or more) enzymatically active
102 domains (EAD) together with a cell wall-binding one (CWBD). Therefore, synthetic
103 biology strategies, such as construction of completely new lysins made up of different
104 modules as "building blocks", have been shown to be achievable. Such strategies enable
105 the design and production of tailor-made antimicrobials, based on the conjunction of
106 diverse functions of interest into a single protein. Functions of interest may include,
107 besides a catalytic activity against the peptidoglycan network (*i.e.*, an antimicrobial
108 activity), an increased stability in complex media (25) or, more typically, a certain
109 tropism towards a specific element on the bacterial surface (26) or some other
110 macromolecules like cellulose (27). The engineering approaches mentioned above have
111 circumvented the alleged inability of lysins to cross the outer membrane (OM) of G−
112 (28, 29). Different kinds of synthetic lysins have been devised to that end. Among them
113 we can mention the so-called 'artilysins', which are lysins fused to different kinds of
114 membrane permeabilizing peptides (30), the 'lysocins', which are lysins fused to
115 elements from bacteriocins that enable bacterial surface recognition and import into the
116 periplasm (22) and the 'innolysins', lysins fused to phage receptor-binding proteins
117 (31).

However, a number of lysins also encompass intrinsic bactericidal activity on G– (32–34). This activity was first noticed for the T4 phage lysozyme (35) and several *Pseudomonas aeruginosa* phage lysins (36). Such unexpected property was attributed to non-enzymatic mechanisms, previously described in partially denatured hen egg-white lysozyme (37), and relies on the presence of antimicrobial peptide (AMP)-like subdomains within such lysins, usually at a C-terminal position (32, 38). Recently, it has been suggested that such AMP-like elements are widespread among lysins from phages infecting G−, and that they might cooperate to host lysis by providing an additional affinity towards the cell wall, because of their high net charge (28, 33, 39–41). Since most lysins from G− are assumed to be monomodular, such AMP-like elements are thought to be an alternative to the CWBDs found in multimodular G+ phage lysins for substrate binding. However, it has not been yet properly examined how widespread this trait would actually be, and, therefore, its true functional and evolutionary implications are largely unknown. Of note, such AMP-like elements have been successfully used to design AMPs active on their own (36, 39, 42).

To uncover the actual evolutionary relevance of these AMP-like elements, as well as other lysin features, such as their domain architecture, in this work, a bioinformatic approach examining a wide collection of lysins has been proposed. There are several precedents on the application of homology-based analysis of putative lysin sequences that have paved the way to the systemic comprehension of the co-evolution of phage lysins and their hosts (13, 43). The present study aims to update the picture with the latest available information, as well as to provide answers to the recent questions brought forward by the lysin engineering literature. Therefore, based on current knowledge on the matter and available genomic data, we have constructed and curated a comprehensive database of phage lysin sequences. Subsequent analyses on the data

included: a) an initial exploration of the database composition; b) a cross reference of information added to the database to check for differential distribution of distinct domain families and their architectural combinations along different bacterial groups; and c) an overview of easily computable physicochemical properties (net charge, hydrophobicity, etc.) along amino acid (aa) sequences to explore widespread, relevant differences between groups. The hereby conclusions shall, then, strengthen our understanding of lysins specificity and variability, and help in future drug design efforts based on phage products.

RESULTS AND DISCUSSION

Outline. A total of 9,539 genomes were prospectively obtained from the National Center for Biotechnology Information (NCBI) database (retrieved on April, 2020). After a careful curation process (for details, see Methods), the final database contained 2,182 proteins and a total of 3,303 Pfam (PF) hits (Table S1 in the supplemental material). Each of these sequences was associated with a bacterial genus corresponding to its described host, for which data on its Gram group and peptidoglycan chemotype was added (Table S2 in the supplemental material). In total, our database comprised phage lysins from 47 bacterial genera, accounting for up to a total of 2,179 sequences, plus three lysin sequences from PRD1-like phages that infect several enterobacteria. Taking into account all of the identical sequences, the 2,182 different sequences of our data set correspond, in fact, to 36,365 entries in the NCBI Reference Sequence database **(**RefSeq; release 202) (44).

General differences among lysins. For 1,512 out of 2,182 sequences (69.3%), only one significant PF hit could be predicted (Fig. 1A). This was especially relevant for lysins from phages infecting G–, given that 90.6% of these proteins were predicted to

contain a single functional domain. Near 60% of the lysins from phages infecting G+ (for the sake of this work, mycobacteria and their relatives like *Rhodococcus* or *Corynebacterium* were included among G+), harboured only one functional domain. Few lysins appear to contain ≥ 4 PF hits (Fig. 1A). However, these figures should be considered with caution since they do not correspond to the number of real functional modules within the protein, but to a relatively high number (up to 5) of individual repeats that, together, make up a single functional module. For example, the 37 sequences with 6 PF hits correspond to streptococcal phage lysins having the typical structure [EAD]5×[*CW_binding_1*], being EAD either *Amidase_2* (31 hits), *Glyco_hydro_25* (3 hits) or *CHAP* (3 hits) domains. Likewise, not all sequences with a single PF hit should be assumed to contain only a single domain since many of them might contain other, still undefined domains. Also, some repeats (or even full domains) might not be appropriately predicted if there is enough evolutionary sequence divergence. As an example, the domain structure based upon the three-dimensional folding of pneumococcal major autolysin LytA (45) does not concur with the domains predicted by an homology search since such method is unable to uncover the latest CWBD repeat (Fig. S1 in the supplemental material).

As a whole, however, the differential relative amount of single and multiple PF hits sequences between G– and G+ phage lysins (Fig. 1A and E) can be taken into account, in accordance with the usual proposal that G– lysins are typically monomodular, while G+ ones are multimodular (46). This is further supported by the evident difference in protein length distributions (Fig. 1B), where G+ phage lysins tend to be larger (median = 317 aa residues) than G– ones (median = 164 aa residues); and also by the differential distribution of sequence lengths before and after the predicted EADs (Fig. 1C and 1D). Fig. 1C shows that EADs from G– phage lysins start, approximately, at the same point

than G+ ones, this is, near to the N-terminal end of the protein, except that the EADs starting point distribution is slightly shifted towards the C-terminal part of the enzyme in lysins from G–, probably due to the presence, in some cases, of CWBDs at the N-terminus (28). Of note, G+ EADs starting point distribution shows a secondary local maximum at around coordinate 200. This is consistent with the presence of EADs at a medial location within the protein, something that has already been observed in many G+ phage lysins (13, 47). According to Fig. 1D, most G+ EAD hits have much more "space" at the C-terminal part than G– ones (respective medians of C-terminal length after EAD hit distributions for G– and G+ are 16 and 136 aa residues). The additional length at the C-terminal part of G+ phage lysins must be occupied by non-catalytic domains (*i.e.*, CWBDs) and, taken together, all this evidence would support the common postulate that most detected G– lysins are monomodular.

Finally, Fig. 1F illustrates that, in contrast with the case of G– lysins, G+ lysins present a high diversity of different types of domains. There is a remarkable predominance of the EADs belonging to the *Phage_lysozyme* family of proteins in G– lysins (45.4% of total hits), whereas *Amidase*_2, the most frequent EAD among G+ phage lysins, accounted only for 22.2% of G+ PF hits.

Differential distribution of domain families among different bacterial host groups. A distribution analysis of each PF family amongst bacterial hosts was performed (Table 1). From the total 3,303 PF hits analysed, 2,460 corresponded to phages infecting G+ bacteria. 2,243 (1,477 G+; 766 G–), 1,054 (982 G+; 72 G–), and 6 (G–) corresponded to EADs, CWBDs, and structural domains, respectively (the sources for domains classification as EAD, CWBD or structural, can be consulted at Table S3 in the supplemental material). When the differential Gram group classification of each PF hit was analyzed, it was found that EADs like *Amidase_5*, *Glyco_hydro_25*,

Peptidase_C39_2, and *Transglycosylase* were exclusive of G+, whereas *Glyco_hydro_108* or *Muramidase* were characteristic of phages infecting G–. Other EADs like *Amidase_2*, *Amidase_3*, *CHAP*, *Glucosaminidase*, *Peptidase_M15_4*, and *Peptidase_M23* were common in G+, whereas *Glyco_hydro_19*, *Hydrolase_2*, *Phage_lysozyme* dominated amongst G–. Besides, *CW_7*, *CW_binding_1*, *LGFP*, *SH3_5*, or *ZoocinA_TRD* constituted the CWBDs of G+, and, although *LysM* and *PG_binding_1* were most frequently found in G+ lysins, also appeared sometimes among G– (Table 1 and Fig. 2). *PG_binding_3* was the only CWBD exclusive of G– lysins. Interestingly, all of the 40 *PG_binding_3* occurrences were accompanied by *Glyco_hydro_108* at the N-terminal moiety, yielding an architecture ([*Glyco_hydro_108*][*PG_binding_3*]) that was widespread among γ-proteobacteria.

Trends in PF domains distribution among genera, rather than Gram group, were a bit more complex (Figs. 3 and 4), although some conclusions could be reached. To begin with G+ CWBDs, the *CW_binding_1* repeats were only encoded by phages infecting streptococci, whereas *CW_7* constitute the CWBD of many phage lysins of *Streptococcus*, *Arthrobacter*, and *Streptomyces*. *CW_binding_1* repeats are known to bind choline residues present in the teichoic acids of *Streptococcus pneumoniae* and its relatives (*i.e.*, streptococci of the Mitis group) (48, 49), and therefore only appeared within our dataset among such group of bacterial hosts (Fig. S2 in the supplemental material). CW_7 repeats are known to bind a conserved peptidoglycan motif, and are thus less restricted in the variety of bacteria they may recognize (50). *LysM* domains were also widely distributed in G+, *ZoocinA_TRD* was very common among *Streptococcus thermophilus* and *PSA_CBD* was exclusive for *Listeria* phage lysins. As for EADs, *Amidase_5* was very frequently found among streptococci and *Amidase_2* generally abundant among all G+.

Another exclusive trait of some G+ lysins was the concurrence of two distinct EADs. This was observed for phage lysins from *Streptococcus suis*, Pyogenic group streptococci, staphylococci or mycobacteria. A possible explanation for multicatalytic lysins is an increased lytic efficiency over monocatalytic ones, since activities attacking different sites of the peptidoglycan are known to act synergistically in peptidoglycan degradation (51). Such synergy could also imply a decreased chance for the appearance of resistant peptidoglycan mutants (52). It has also been shown that the synergistic concurrence of both activities is sometimes needed for full activity. Thus, it has been suggested that some phages may have evolved a regulatory mechanism to avoid lysis of other potential host cells relying on the proteolysis of bicatalytic lysins by host-cell proteases. Then, both EADs would be disjointed by proteolysis upon host cell lysis and the degraded lysins would no longer be active against the nearby bacterial population (53). This should be especially relevant for phages infecting G+ bacteria, which lack a protective OM hindering the lysis of other bacterial cells from without, and hence the exclusiveness of the bicatalytic architecture among phages infecting G+. In some other cases, however, it is the high affinity of the CWBD that has been proposed as the mechanism that maintains lysins tightly bound to cell debris preventing widespread lysis of the bacterial community (54), which is also an argument for the widespread presence of CWBDs among G+ and not among G–.

Staphylococcal phage lysins presented reduced EAD variability, normally using *Amidase_2*, *Amidase_3* and/or *CHAP* domains, with *SH3B_5* being the preferred CWBD, in agreement with previous results (55). In some cases, the staphylococcal *SH3B_5* has been shown to bind the peptidoglycan with the characteristic pentaglycine interpeptidic bridge of *Staphylococcus* (56). Domains putatively assigned an esterase activity (*Cutinase*, *FSH1*, *PE-PPE*) were only present in phages from *Mycobacterium*

and its relatives, presumably as type B lysins. The *LGFP* repeats, quite common among *Rhodococcus* phages, might be a specific CWBD among such Corynebacteriales. Peptidase EADs were common and diverse among mycobacteriophages, in contrast with other G+ phages, which do not typically contain peptidase EADs other than *CHAP*. Of note, *CHAP* domains have been sometimes described as peptidases but, in other occasions, as *N*-acetylmuramoyl-L-alanine amidases (NAM-amidases) (57, 58).

Regarding G–, the most widely spread architecture of G– phage lysins was monomodular, harbouring a single *Phage_lysozyme* domain, which accounted for half (50.8%) of the identified G– lysins in our database. Another architecture that was only found in G– lysins is the localization of a CWBD at N-terminal end (for example, as [*PG_binding_1*] [*Muramidase*]), although they were not at such position in every case (*e.g.*, architecture [*Glyco_hydro_108*] [*PG_binding_3*] was also present).

The correlation between domain distribution and peptidoglycan composition might also shed some light on the relationships of different domain families with different taxa. To that end, the chemotypes classification of peptidoglycan proposed by Schleifer and Kandler (59) was used (Table S2 in the supplemental material). Briefly, such classification hierarchically relies on (i) the site of cross-linkage of the peptide subunit of the peptidoglycan, (ii) the nature of the cross-link and (iii) the specific residue at position 3 within such peptide subunit (Fig. 5A). Starting by CWBDs (Fig. 5B), classification by chemotypes did not provide a better explanation for specificity than other genera-specific traits, as discussed above. Some specificities could be found though (*e.g.*, *Amidase02_C* appears only in phages that infect A1α bacteria or *PG_binding_3* only in A1γ), and some CWBDs that are widespread among different chemotypes could also be observed (*PG_binding_1*, *LysM*, *SH3_5*). In general, however, it cannot be stated that peptidoglycan composition is a major determinant for

CWBD specificity, except for some cases such as, for example, *ZoocinA_TRD* domains, which has been proposed to bind A3α with two Ala residues at the cross-link (60). The poor performance of chemotype as an *a priori* predictor of the CWBD PF family ligand is more clearly evident if we consider the CWBD types which appeared widespread among many different chemotypes, such as *LysM* and *SH3_5*. To check whether this apparent 'promiscuity' may be linked to the presence of subfamilies with potentially different ligands or if it could rather be a true promiscuous binding, SSNs were constructed with the PF hits of *LysM* and *SH3_5* (Fig. S3 in the supplemental material). The *LysM* SSNs did not show prominent similarity clusters either classified by taxon or by chemotype of the bacterial host. This suggests that *LysM* could be a truly 'universal' CWBD that would bind to a conserved cell wall ligand. The rather generic description of *LysM* ligands in the literature (as 'N-acetylglucosamine-containing polysaccharides') is in agreement with this observation. *SH3_5*, however, displayed at least two differentiated sequence similarity groups that correlated rather well with different taxonomic groups (namely, staphylococci versus streptococci and lactobacilli). In fact, literature reflects that, while lytic enzymes with predicted *SH3_5* domains typically recognize polysaccharides (and peptidoglycan in particular), there seem to be different specializations. For example, the CWBD of the *Lactiplantibacillus plantarum* major autolysin binds many different peptidoglycans with low affinity, being glucosamine the minimal binding motif (61), while *SH3_5* domains from staphylolytic enzymes have been shown to be rather specific to crosslinked peptidoglycans (like the A3α peptidoglycan of *Staphylococcus* and *Streptococcus*) and that the nature of the crosslink itself determines the affinity of such CWBDs for the peptidoglycan (62, 63).

Additional information could be drawn from this analysis when applied to the different catalytic activities detected (Fig. 5C). First of all, NAM-amidases were the

most represented type of domains and also those that appeared among more different taxonomic groups and chemotypes, even more so than lysozymes. Indeed, *Amidase_2*, the most abundant PF domain in our dataset (638 hits), appeared both in lysins from G+ and G− phages. The SSN in Fig. S3 in the supplemental material shows, however, that although *Amidase_2* seems a rather diverse group, with various observable similarity clusters, none of such clusters correlate with any of the classifiers of the bacterial hosts tested.

Muramidases were quite overrepresented among G– bacteria (chemotype A1γ) because of the widespread presence of *Phage_lysozyme* domains. Glucosaminidases appeared evenly both against A1 and A3 peptidoglycans, but whereas in G+ bacteria (which comprise all A3s and a few A1s) glucosaminidase activity was represented by *Glucosaminidase* PF domain, the only domain putatively assigned with a glucosaminidase activity among G– was *Glyco_hydro_19* (Figs. 3 and 5).

Another interesting remark is that peptidase activities were more common amongst lysins from phages infecting bacteria with subgroup A1 peptidoglycans which, in turn, display the simplest cross-linkage of all types, lacking an interpeptide bridge. Thus, peptidases were not uncommon among G–, and were also present in A1 phages from G+ (especially mycobacteriophages, but also listeriophages and phages from *Clostridium*, *Bacillus* or *Corynebacterium*). On the other hand, amidase/peptidases, which is the label given to *CHAP* domains (Table S3 in the supplemental material), were much more prevalent among A3 G+, and only seldom present in lysins from phages infecting A1 bacteria (namely some G–). This suggests that if there was to be an A3-specific peptidase activity would be that located in *CHAP* domains. It makes sense that different peptidase structures have evolved towards A1 and A3 peptidoglycans, since the complexity of their peptidoglycan peptide moieties differs significantly.

343 Adding to this conclusion, the *CHAP* SSN (Fig. S3 in the supplemental material) did
344 show a similarity clustering of the few *CHAP* examples in lysins from A1 phages,
345 besides an apparent differentiation of *Staphylococcus* and *Streptococcus*/*Enterococcus*.

346 **Physicochemical analysis of phage lysins from Gram-positive *versus* those from**
347 **Gram-negative bacteria.** The results analysed so far support a distinct distribution of
348 domain architectures and families among lysins that infect different kinds of bacteria,
349 and even hint to an association of such differential distribution to some cell wall
350 properties. To check whether such variations can also be correlated with a measurable
351 difference in physicochemical properties, net charge, net charge per residue (NCPR),
352 hydrophobicity, average hydrophobic moment, and aliphatic index were calculated and
353 used to implement a random forest (Fig. 6). This way, the aforementioned
354 physicochemical variables were used as classifiers for the prediction of the host
355 bacterium Gram group of lysins. The resulting algorithm yielded a Receiver Operating
356 Characteristic (ROC) plot with an area under the curve (AUC) of 0.897, which can be
357 interpreted as a good predictive ability (Fig. 6A). Using the probability threshold
358 (0.591) derived from the best point of the ROC curve (which maximizes true positive
359 rate and minimizes false positive rate), G+/G− classification upon the testing subset
360 (Fig. 6B) managed an accuracy of 87.9% with sensitivity and specificity, respectively,
361 of 84.1% and 81.3% (being the classification as G+ the "positive" one). According to
362 the subsequent analysis (Fig. 6C), NCPR was the most relevant variable to distinguish
363 between G+ and G–, followed by average hydrophobic moment and aliphatic index and,
364 finally, hydrophobicity. In general, these results suggest that lysins from phages that
365 infect G+ and G– can in fact be differentiated by their physicochemical properties in a
366 relatively efficient manner. For visualization of the differences between G+ and G−, a
367 multidimensional scaling (MDS) plot based on the proximity matrix from the random

forest model was drawn (Fig. 6D). Such plot showed the clustering of G− lysins within the 2-dimensional space based on the physicochemical variables, while G+ ones seemed to be more dispersed. A qualitative interpretation of this result may reflect the aforementioned wide diversity of functional modules and architectures of G+ lysins (Fig. 1D, Fig. 4) in contrast with the relatively low variability of G−. Such low variability of the G− lysins hereby analysed would then be associated with a preference for some physicochemical features. The sense of this preference was subsequently checked.

Indeed, the net charge distribution (normalized by protein length) was significantly higher in G− lysins than in G+ ones ($p \leq 0.0001$; ES = 0.66) (Fig. 7A, most left panel). Moreover, the average prediction of local net charge suggested that such difference is mainly located at the C-terminal part of G− lysins (Fig. 7B). A more thorough comparison (Fig. 7C) seemed to confirm this. At every sequence quartile of the proteins (*i.e.*, contiguous fragments of sequence with a length equal to 1/4 of the total number of aa residues in the original protein sequence), the net charge distribution of G− lysins had a significantly higher net charge. However, the actual size of this shift was only moderate along the sequences (ES between 0.24 and 0.34) but it was, again, higher at the final quartile (0.52).

Hydrophobicity was also higher in G– lysins, but the difference regarding G+ ones is smaller ($\zeta = 0.36$). This might be related to the rather inconsistent pattern shown by average local hydrophobicity and sequence quartiles comparison (Fig. 7BC). G– lysins tended to have a more hydrophobic N-terminal part, whereas at the C-terminal moiety the tendency was reversed, something that can be explained by the relative abundance of positively charged residues shown before for G–. It is at the third quartile (Q3), immediately before the high positive net charge patch described above, where the

393 difference was statistically more relevant ($p \leq 0.001$; ES = 0.59), with higher values in
394 G–s. There was also a statistically significant difference in the average hydrophobic
395 moment distributions between G+ and G– phage lysins. For the G– group, the local plot
396 (Fig. 7B) showed a higher tendency to present greater hydrophobic moments along the
397 whole protein length but the N-terminal part. Analysis of sequence quartiles confirmed
398 a statistically significant superiority of average hydrophobic moment for G– except at
399 N-terminal. The aliphatic index was also significantly higher in G–, although G+
400 showed an aliphatic index peak at their C-terminal part that surpassed that of G–
401 (coincidental with G– basic aa peak, which, understandably, would lower both
402 hydrophobicity and aliphatic index at Q4) (Fig. 7C).

403 Taking all these observations together with the results thrown by the random forest
404 prediction, we can conclude that the physicochemical difference between lysins from
405 phages that infect G+ or G– bacteria is specified as a higher positive net charge of G–,
406 particularly at C-terminal end, combined with a greater propensity in incorporating
407 aliphatic aa and likely resulting in amphiphilic structures.

408 A closer examination of net charge (and C-terminal net charge) of lysins from G–
409 infecting phages indicated that the high positive patch trait seems specific to some
410 domain families. As a whole, a statistically significant higher NPRC value was found in
411 lysins bearing *Phage_lysozyme*, *Hydrolase_2* and *Glyco_hydro_19* domain families
412 (Fig. 8). At the C-terminal part, higher NCPR was found in lysins bearing the same
413 domains mentioned above, but also in *SLT* and *Muramidase*. The average local net
414 charge tendency showed for each EAD group (Fig. S4 in the supplemental material)
415 confirmed that a local high positive charge peak appears in the protein part immediately
416 before the C-terminal apex.

Interestingly, all of the aforementioned domains that present a higher, positive charge patches at their C-terminal part were preferentially present in lysins from phages that infect G– bacteria (Table 1). This observation provides a basis to argue a generalized evolutionary tendency in G– infecting phages towards developing AMP-like subdomains at the C-terminal moiety of their lysins. Such subdomains contain, indeed, features typical of AMPs (such as the high net charge accompanied by a high local hydrophobic moment, hydrophobic patches, etc.), and may play a role in the interaction between lysins and cell wall in G– bacteria. Electrostatic interactions do play a significant role in phage-bacteria interplay, as suggested for modular lysins from phages that infect G+ bacteria. For example, it has been shown that the negative net charge of many G+ lysins hinders their ability to approach the negatively charged cell wall (18, 64). This renders the affinity-based interaction of the CWBDs with their cell wall ligands essential for lysins activity. This essentiality of CWBDs has been shown for several lysins (20), but generalizations should be made with caution because there are also cases reported of single catalytic domains that lysed G+ cells more efficiently when their CWBD was removed (65). To our knowledge there are only few cases reported in which CWBDs appear to increase the efficiency of cell wall-lysin interaction in G– lysins (21). We have already shown, based on our own data, that it is safe to say that G– lysins are monomodular. Thus, taking this theoretical framework into account, it could be argued that G– lysins should have evolved a distinct strategy to grant cell wall interaction, namely an increased net charge and, perhaps, the presence of hydrophobic patches near such basic residues (*i.e.*, AMP-like regions), rather than containing an additional CWBD, which, incidentally, might be essential for post-lytic regulation in G+, but not in G– (54). The AMP-like subdomains, besides providing better anchorage to bacterial surface structures, might as well act as an additional mechanism towards

effective lysis of G– bacteria. There are indeed abundant examples in literature on the ability of G– lysins to interact with the OM and permeabilize it (33, 38, 39, 66), a trait that, it is plausible to say both from our own analysis and the experimental results of many works, would reside in such AMP-like elements. If we assume this, the identification of AMP-like subdomains within lysins could provide also a way of predicting the ability of such lysins to better interact with the OM from without, and thus their antimicrobial potential.

Concluding remarks. Phages and their bacterial hosts are constantly evolving in a co-dependent manner (67). From the point of view of phage lysins, this means that such molecules have adapted to the particular structures and features of the host cells. This adaptation can be described as the functional adjustment of the protein elements to optimally fulfil their purposes: the efficient and regulated degradation of the peptidoglycan. Therefore, lysin structures and cell wall structures must be closely correlated. A way of testing and understanding such relationship was the hereby presented sequence-based classification of the domains constituent of phage lysins, and the analysis of their distribution among (pseudo)taxonomical and structural classes of bacterial hosts. Our procedure yielded several important associations of lysins and cell wall architectures explainable in a structural-functional way:

a) The different architectures found between lysins from phages that infect G+ or G–. The ones from G– are usually monomodular, whereas lysins from G+ infecting phages are multimodular. Moreover, the bicatalytic type of modular structure only appears among G+. An explanation for this architecture is the requirement for a tighter post-lytic regulation in G+ and/or a more efficient lytic activity relying on a tighter substrate binding or on the synergistic effect of combining different catalytic activities.

b) The association of CWBDs with specific bacterial host genera in our dataset, together with the literature showing that many of these CWBDs are able to recognize ligands that are specific traits of the related bacterial hosts. For example, *SH3_5* in staphylococcal phages, *CW_binding_1* in *Streptococcus* Mitis group phages, *PSA_CBD* in listeriophages, or *PG_binding_3* in G–. This also manifests the genetic trading between host and parasite, since many of those CWBDs, as well as their bacterial ligands, are also used by the bacterial host surface proteins.

c) The differential appearance of EAD families within phages that infect bacteria with a certain chemotype, which suggests an adaptation of the enzyme to the structure of the specific peptidoglycan it has to degrade. This is notable in the case of peptidases. The somewhat wide range of peptidases identified within our data set is mainly distributed among phages infecting bacteria with subtype A1 peptidoglycan. In phages that infect subtype A3 bacteria, the most common EAD is *CHAP*, which has been shown to function either as NAM-amidase or as endopeptidase, in any case, specific for A3 peptidoglycan.

d) The remarkably differential distribution of domain families among phages that infect either G+ or G–, together with the association of such domains with different physicochemical properties.

e) The differential physicochemical properties between lysins from G+ and G– that, conversely, allows to predict the Gram group of the bacterial host of a given lysin based on its sequence. In this work, the trait of a positively charged patch at a C-terminal position was found to be widespread among lysins from G– bacteria infecting phages. Such trait has been previously related with an improved ability to interact with the G– OM, and might be a ‘substitutive’ of the

typical G+ CWBDs. The higher values of other physicochemical variables in G– (aliphatic index, hydrophobic moment) also suggest an analogy of certain structural segments of G– lysins with AMPs.

These observations have clear implications on the design and development of lysin-based antimicrobials, from rational search (or design) of novel lysin parts to deriving AMPs from lysins sequences. A possible setup in which specific bacterial infections are tackled in a personalized manner based on a knowledge-driven, highly efficient synthetic biology platform for lysin-based antimicrobials production can be envisioned in a near future. The conclusions of this work can contribute to the consolidation of such a framework, together with the cutting-edge research currently being carried out in the field.

METHODS

Sequence database construction and curation. Phage genomes were retrieved from NCBI nucleotide database by searching phage complete genomes constrained to several bacterial taxa of interest, mainly selected by clinical or epidemiological importance and availability. Those genomes were screened for gene products whose annotations could suggest them to be lytic enzymes. Therefore, keywords such as 'lysin', 'lysozyme', 'murein', 'amidase', 'cell wall hydrolase', 'peptidase' or 'peptidoglycan' were used as inclusion criteria, while 'structural', 'tail', 'holin', 'baseplate' or 'virion protein' were used as exclusion terms to try and avoid misidentifications. Associated information such as taxon of the bacterial host, aa sequence, annotations, phage denomination, and protein/genome unique identifiers were also added into the database.

Curation included: 1) a sequence length cutoff, established with a minimum of 50 and a maximum of 550 aa residues; 2) a sequence identity cutoff using CD-HIT (68) with default parameters and a 98% identity cutoff value to avoid redundant entries; 3) examination with PfamScan (expectation value cutoff = 10) (69, 70) to rule out sequences where no relevant significant hits were found (*i.e.*, where no functional domains that would plausibly appear within phage lysins were detected); 4) bacterial host

519 genus assignation to each entry based on literature and genome annotations). The complete lysins
520 collection and PF hits are available as Table S1 in the supplemental material and at Digital.CSIC (71).

521 **Physicochemical properties prediction and analysis.** Prediction of physicochemical properties (net
522 charge, aliphatic index, hydrophobicity, hydrophobic moment) based on the aa sequences retrieved were
523 performed using the R package 'Peptides' implementation (72). Dawson's pK_a scale was used for
524 prediction of net charge assuming pH = 7.0 (73); hydrophobicity scale was that proposed by Kyte and
525 Doolittle (74) and hydrophobic moment was calculated as previously proposed (75) with a specified
526 rotational angle of 100° (recommended angle for α-helix structures). An average value of the hydrophobic
527 moment of each of the possible 11-aa helices within a given sequence is given whenever noted. Such
528 properties were predicted in the whole sequences, in sequences quartiles (contiguous fragments of
529 sequences that account in length each for a quarter of the whole sequence) or in peptides of 11 aa length
530 to provide either a global vision or more local information.

531 A random forest algorithm was used to check the ability of physicochemical properties to predict lysin
532 sequences as from a G+ or G– infecting phage. R package 'caret' was employed for creating, fitting and
533 testing the random forest, and further analyses on the model (ROC curve, MDS plotting) were performed
534 using packages 'pROC' and 'randomForest'. The dataset was randomly partitioned into a training subset
535 (75% of all entries) and a testing subset. The training subset was used to fit the random forest parameters
536 (namely, the randomly selected variables for each node, which was fixed in 4) by a 5-fold cross-
537 validation with 3 repeats. Then the constructed random forest was validated using the previously defined
538 testing subset.

539 **Sequence similarity networks.** SSNs were generated for visually assessing the similarity clustering
540 of sequence sets. For this purpose, the Enzyme Similarity Tool from the Enzyme Function Initiative
541 server (EFI-EST) was employed (76). Briefly, this tool performs a local alignment from which every
542 possible pair of sequences receives a score similar to the E-value obtained from a typical BLAST
543 analysis. A threshold score value was selected for each SSN so that below such threshold sequence pairs
544 were considered nonsimilar and, therefore, the pair would not be connected in the resulting
545 representation. Scores were selected so that sequence pairs whose similarity was below 30-40% were
546 deemed non-similar. The SSN graphs were produced Cytoscape 3 with yFiles organic layout (77).

547 **Statistical analysis.** Default methods for data representation implemented in 'ggplot2' R package
548 such as kernel density estimation or GAM smoothing were used throughout this work for data

visualization (78). For comparison of non-normal, heteroskedastic data populations, robust statistical methods were used (79). Specifically, a generalization of Welch's test with trimmed means (default trimming level $\gamma = 0.20$) was used with Bonferroni adjustment when multiple comparisons were performed. Effect sizes were estimated according to Wilcox and Tian's ζ (80). A general interpretation for ζ is given in the previous reference, being values of around 0.10 a small effect size, around 0.30 a medium effect and 0.50 and above a large one. A p-value ≤ 0.05 was considered significant. All robust methods were used from the implementation in R Package 'WRS2' (81).

Data Availability. All data used throughout this work are available at Digital.CSIC repository (http://hdl.handle.net/10261/221469) and in Supplemental Material.

SUPPLEMENTAL MATERIAL

TABLE S1. Accession numbers, sequences and PF domains predicted for the lysins data set constructed in this work.

TABLE S2. Traceability information and yield of the curation process.

FIG S1. Schematic architecture of the LyA autolysin of *S. pneumoniae*.

TABLE S3. Information on the PF families found within the lysins sequences database.

FIG S2. Heatmap depicting PF hits distribution among different streptococci.

FIG S3. Sequence similarity networks (SSNs) of the PF hits in our dataset corresponding to different domain families.

FIG S4. Local computation of physicochemical properties in lysins from G– infecting phages classified according to EAD predictions.

ACKNOWLEDGMENTS

This study was funded by a grant from the Ministerio de Economía y Competitividad (MINECO-FEDER, SAF2017-88664-R). Additional funding was provided by the Centro de Investigación Biomédica en Red de Enfermedades Respiratorias (CIBERES), an initiative of the Instituto de Salud Carlos III. Roberto Vázquez was the recipient of a predoctoral fellowship from CIBERES.

The authors gratefully acknowledge Guillermo Padilla for his fundamental advice in statistical data treatment and representation.

The authors have declared that no competing interests exist.

Authors contribution statement: RV and PG conceptualization; RV performed the analysis and constructed the database; RV and EG data curation; RV wrote the original draft of the paper; all authors read, edited and approved the final manuscript.

REFERENCES

1. Silver LL. 2011. Challenges of antibacterial discovery. Clin Microbiol Rev 24:71-109.
2. Sabtu N, Enoch DA, Brown NM. 2015. Antibiotic resistance: what, why, where, when and how? Brit Med Bull 116:105-113.
3. European Antimicrobial Resistance Surveillance Network (EARS-Net). 2919. Surveillance of antimicrobial resistance in Europe 2018.
4. Centers for Disease Control and Prevention. 2019. Antibiotic resistance threats in the United States 2019.
5. Hofer U. 2019. The cost of antimicrobial resistance. Nat Rev Microbiol 17:3.
6. Organisation for Economic Co-operation and Development. 2018. Stemming the superbug tide: just a few dollars more.
7. Tacconelli E, Carrara E, Savoldi A, Harbarth S, Mendelson M, Monnet DL, Pulcini C, Kahlmeter G, Kluytmans J, Carmeli Y, Ouellette M, Outterson K, Patel J, Cavaleri M, Cox EM, Houchens CR, Grayson ML, Hansen P, Singh N, Theuretzbacher U, Magrini N, the WHO Pathogens Priority List Working Group. 2018. Discovery, research, and development of new antibiotics: the WHO priority list of antibiotic-resistant bacteria and tuberculosis. Lancet Infect Dis 18:318-327.
8. O'Neill. 2016. Tackling drug-resistant infections globally: final report and recommendations. The review of antimicrobial resistance (https://amr-review.org/sites/default/files/160525_Final%20paper_with%20cover.pdf).
9. Theuretzbacher U, Outterson K, Engel A, Karlén A. 2020. The global preclinical antibacterial pipeline. Nat Rev Microbiol 18:275-285.
10. McCallin S, Sacher JC, Zheng J, Chan BK. 2019. Current state of compassionate phage therapy. Viruses 11:343.
11. Abdelkader K, Gerstmans H, Saafan A, Dishisha T, Briers Y. 2019. The preclinical and clinical progress of bacteriophages and their lytic enzymes: the parts are easier than the whole. Viruses 11:96.
12. Young R. 2014. Phage lysis: three steps, three choices, one outcome. J Microbiol 52:243-258.
13. Payne KM, Hatfull GF. 2012. Mycobacteriophage endolysins: diverse and modular enzymes with multiple catalytic activities. PLoS One 7:e34052.
14. Kongari R, Rajaure M, Cahill J, Rasche E, Mijalis E, Berry J, Young R. 2018. Phage spanins: diversity, topological dynamics and gene convergence. BMC Bioinformatics 19:326.
15. Dams D, Briers Y. 2019. Enzybiotics: enzyme-based antibacterials as therapeutics. Adv Exp Med Biol 1148:233-253.
16. Pastagia M, Schuch R, Fischetti VA, Huang DB. 2013. Lysins: the arrival of pathogen-directed anti-infectives. J Med Microbiol 62:1506-1516.
17. Cheng M, Zhang Y, Li X, Liang J, Hu L, Gong P, Zhang L, Cai R, Zhang H, Ge J, Ji Y, Guo Z, Feng X, Sun C, Yang Y, Lei L, Han W, Gu J. 2017. Endolysin LysEF-P10 shows potential as an alternative treatment strategy for multidrug-resistant *Enterococcus faecalis* infections. Sci Rep 7:10164.
18. Díez-Martínez R, de Paz HD, Bustamante N, García E, Menéndez M, García P. 2013. Improving the lethal effect of Cpl-7, a pneumococcal phage lysozyme with broad

bactericidal activity, by inverting the net charge of its cell wall-binding module. Antimicrob Agents Chemother 57:5355-5365.

19. Kusuma C, Jadanova A, Chanturiya T, Kokai-Kun JF. 2007. Lysostaphin-resistant variants of *Staphylococcus aureus* demonstrate reduced fitness in vitro and in vivo. Antimicrob Agents Chemother 51:475-482.
20. Vázquez R, García E, García P. 2018. Phage lysins for fighting bacterial respiratory infections: a new generation of antimicrobials. Front Immunol 9:2252.
21. Gerstmans H, Criel B, Briers Y. 2018. Synthetic biology of modular endolysins. Biotechnol Adv 36:624-640.
22. Heselpoth RD, Euler CW, Schuch R, Fischetti VA. 2019. Lysocins: bioengineered antimicrobials that deliver lysins across the outer membrane of Gram-negative bacteria. Antimicrob Agents Chemother 63:e00342-19.
23. Diaz E, López R, Garcia JL. 1991. Chimeric pneumococcal cell wall lytic enzymes reveal important physiological and evolutionary traits. J Biol Chem 266:5464-5471.
24. Gerstmans H, Grimon D, Gutiérrez D, Lood C, Rodríguez A, van Noort V, Lammertyn J, Lavigne R, Briers Y. 2020. A VersaTile-driven platform for rapid hit-to-lead development of engineered lysins. Sci Adv 6:eaaz1136.
25. Seijsing J, Sobieraj AM, Keller N, Shen Y, Zinkernagel AS, Loessner MJ, Schmelcher M. 2018. Improved biodistribution and extended serum half-life of a bacteriophage endolysin by albumin binding domain fusion. Front Microbiol 9:2927.
26. Díez-Martínez R, De Paz HD, García-Fernández E, Bustamante N, Euler CW, Fischetti VA, Menendez M, García P. 2015. A novel chimeric phage lysin with high *in vitro* and *in vivo* bactericidal activity against *Streptococcus pneumoniae*. J Antimicrob Chemother 70:1763-1773.
27. Abouhmad A, Mamo G, Dishisha T, Amin MA, Hatti-Kaul R. 2016. T4 lysozyme fused with cellulose-binding module for antimicrobial cellulosic wound dressing materials. J Appl Microbiol 121:115-125.
28. Ghose C, Euler CW. 2020. Gram-negative bacterial lysins. Antibiotics (Basel) 9:74.
29. Briers Y, Lavigne R. 2015. Breaking barriers: expansion of the use of endolysins as novel antibacterials against Gram-negative bacteria. Future Microbiol 10:377-390.
30. Briers Y, Walmagh M, Van Puyenbroeck V, Cornelissen A, Cenens W, Aertsen A, Oliveira H, Azeredo J, Verween G, Pirnay J-P, Miller S, Volckaert G, Lavigne R. 2014. Engineered endolysin-based "Artilysins" to combat multidrug-resistant Gram-negative pathogens. mBio 5:e01379.
31. Zampara A, Sørensen MCH, Grimon D, Antenucci F, Vitt AR, Bortolaia V, Briers Y, Brøndsted L. 2020. Exploiting phage receptor binding proteins to enable endolysins to kill Gram-negative bacteria. Sci Rep 10:12087.
32. Morita M, Tanji Y, Orito Y, Mizoguchi K, Soejima A, Unno H. 2001. Functional analysis of antibacterial activity of *Bacillus amyloliquefaciens* phage endolysin against Gram-negative bacteria. FEBS Lett 500:56-59.
33. Guo M, Feng C, Ren J, Zhuang X, Zhang Y, Zhu Y, Dong K, He P, Guo X, Qin J. 2017. A novel antimicrobial endolysin, LysPA26, against *Pseudomonas aeruginosa*. Front Microbiol 8:293.
34. Lood R, Winer BY, Pelzek AJ, Diez-Martinez R, Thandar M, Euler CW, Schuch R, Fischetti VA. 2015. Novel phage lysin capable of killing the multidrug-resistant Gram-negative bacterium *Acinetobacter baumannii* in a mouse bacteremia model. Antimicrob Agents Chemother 59:1983-1991.
35. Düring K, Porsch P, Mahn A, Brinkmann O, Gieffers W. 1999. The non-enzymatic microbicidal activity of lysozymes. FEBS Lett 449:93-100.
36. Rotem S, Radzishevsky I, Inouye RT, Samore M, Mor A. 2006. Identification of antimicrobial peptide regions derived from genomic sequences of phage lysins. Peptides 27:18-26.
37. Ibrahim HR, Higashiguchi S, Koketsu M, Juneja LR, Kim M, Yamamoto T, Sugimoto Y, Aoki T. 1996. Partially unfolded lysozyme at neutral pH agglutinates and kills

Gram-negative and Gram-positive bacteria through membrane damage mechanism. J Agric Food Chem 44:3799-3806.

38. Orito Y, Morita M, Hori K, Unno H, Tanji Y. 2004. *Bacillus amyloliquefaciens* phage endolysin can enhance permeability of *Pseudomonas aeruginosa* outer membrane and induce cell lysis. Appl Microbiol Biotechnol 65:105-109.

39. Thandar M, Lood R, Winer BY, Deutsch DR, Euler CW, Fischetti VA. 2016. Novel engineered peptides of a phage lysin as effective antimicrobials against multidrug-resistant *Acinetobacter baumannii*. Antimicrob Agents Chemother 60:2671-2679.

40. Maciejewska B, Źrubek K, Espaillat A, Wiśniewska M, Rembacz KP, Cava F, Dubin G, Drulis-Kawa Z. 2017. Modular endolysin of *Burkholderia* AP3 phage has the largest lysozyme-like catalytic subunit discovered to date and no catalytic aspartate residue. Sci Rep 7:14501.

41. Sykilinda NN, Nikolaeva AY, Shneider MM, Mishkin DV, Patutin AA, Popov VO, Boyko KM, Klyachko NL, Miroshnikov KA. 2018. Structure of an *Acinetobacter* broad-range prophage endolysin reveals a C-terminal α-helix with the proposed role in activity against live bacterial cells. Viruses 10:309.

42. Peng S-Y, You R-I, Lai M-J, Lin N-T, Chen L-K, Chang K-C. 2017. Highly potent antimicrobial modified peptides derived from the *Acinetobacter baumannii* phage endolysin LysAB2. Sci Rep 7:11477.

43. Oliveira H, Melo LD, Santos SB, Nobrega FL, Ferreira EC, Cerca N, Azeredo J, Kluskens LD. 2013. Molecular aspects and comparative genomics of bacteriophage endolysins. J Virol 87:4558-4570.

44. Sayers EW, Beck J, Brister JR, Bolton EE, Canese K, Comeau DC, Funk K, Ketter A, Kim S, Kimchi A, Kitts PA, Kuznetsov A, Lathrop S, Lu Z, McGarvey K, Madden TL, Murphy TD, O'Leary N, Phan L, Schneider VA, Thibaud-Nissen F, Trawick BW, Pruitt KD, Ostell J. 2020. Database resources of the National Center for Biotechnology Information. Nucleic Acids Res 48:D9-D16.

45. Li Q, Cheng W, Morlot C, Bai X-H, Jiang Y-L, Wang W, Roper DI, Vernet T, Dong Y-H, Chen Y, Zhou C-Z. 2015. Full-length structure of the major autolysin LytA. Acta Crystallogr Sect D Biol Crystallogr 71:1373-1381.

46. Lai WCB, Chen X, Ho MKY, Xia J, Leung SSY. 2020. Bacteriophage-derived endolysins to target gram-negative bacteria. Int J Pharm 589:119833.

47. Oliveira H, Melo LDR, Santos SB, Nóbrega FL, Ferreira EC, Cerca N, Azeredo J, Kluskens LD. 2013. Molecular aspects and comparative genomics of bacteriophage endolysins. J Virol 87:4558-4570.

48. Fernández-Tornero C, López R, García E, Giménez-Gallego G, Romero A. 2001. A novel solenoid fold in the cell wall anchoring domain of the pneumococcal virulence factor LytA. Nat Struct Biol 8:1020-1024.

49. Fernández-Tornero C, Ramón A, Fernández-Cabrera C, Giménez-Gallego G, Romero A. 2002. Expression, crystallization and preliminary X-ray diffraction studies on the complete choline-binding domain of the major pneumococcal autolysin. Acta Crystallogr Section D, Biol Crystallogr 58:556-558.

50. Bustamante N, Iglesias-Bexiga M, Bernardo-García N, Silva-Martín N, García G, Campanero-Rhodes MA, García E, Usón I, Buey RM, García P, Hermoso JA, Bruix M, Menéndez M. 2017. Deciphering how Cpl-7 cell wall-binding repeats recognize the bacterial peptidoglycan. Sci Rep 7:16494.

51. Vázquez R, García P. 2019. Synergy between two chimeric lysins to kill *Streptococcus pneumoniae*. Front Microbiol 10:1251.

52. Rodríguez-Rubio L, Martínez B, Rodríguez A, Donovan DM, Götz F, García P. 2013. The phage lytic proteins from the *Staphylococcus aureus* bacteriophage vB_SauS-phiIPLA88 display multiple active catalytic domains and do not trigger staphylococcal resistance. PLoS One 8:e64671.

53. Oechslin F, Menzi C, Moreillon P, Resch G. 2018. Post-lytic regulation of bacteriophage lysins explain complex multi-domain architecture and prevents lysis of

neighboring bacterial cell. 2nd International Symposium on Antimicrobial Hydrolytic Enzymes (New York).

54. Loessner MJ, Kramer K, Ebel F, Scherer S. 2002. C-terminal domains of *Listeria monocytogenes* bacteriophage murein hydrolases determine specific recognition and high-affinity binding to bacterial cell wall carbohydrates. Mol Microbiol 44:335-349.

55. Oliveira H, Sampaio M, Melo LDR, Dias O, Pope WH, Hatfull GF, Azeredo J. 2019. Staphylococci phages display vast genomic diversity and evolutionary relationships. BMC Genomics 20:357.

56. Lu JZ, Fujiwara T, Komatsuzawa H, Sugai M, Sakon J. 2006. Cell wall-targeting domain of glycylglycine endopeptidase distinguishes among peptidoglycan cross-bridges. J Biol Chem 281:549-558.

57. Bateman A, Rawlings ND. 2003. The CHAP domain: a large family of amidases including GSP amidase and peptidoglycan hydrolases. Trends Biochem Sci 28:234-237.

58. Rossi P, Aramini JM, Xiao R, Chen CX, Nwosu C, Owens LA, Maglaqui M, Nair R, Fischer M, Acton TB, Honig B, Rost B, Montelione GT. 2009. Structural elucidation of the Cys-His-Glu-Asn proteolytic relay in the secreted CHAP domain enzyme from the human pathogen *Staphylococcus saprophyticus*. Proteins 74:515-519.

59. Schleifer KH, Kandler O. 1972. Peptidoglycan types of bacterial cell walls and their taxonomic implications. Bacteriol Rev 36:407-477.

60. Chen Y, Simmonds RS, Timkovich R. 2013. Proposed docking interface between peptidoglycan and the target recognition domain of zoocin A. Biochem Biophys Res Commun 441:297-300.

61. Beaussart A, Rolain T, Duchene MC, El-Kirat-Chatel S, Andre G, Hols P, Dufrene YF. 2013. Binding mechanism of the peptidoglycan hydrolase Acm2: low affinity, broad specificity. Biophys J 105:620-629.

62. Lu JZ, Fujiwara T, Komatsuzawa H, Sugai M, Sakon J. 2006. Cell wall-targeting domain of glycylglycine endopeptidase distinguishes among peptidoglycan cross-bridges. J Biol Chem 281:549-558.

63. Grundling A, Schneewind O. 2006. Cross-linked peptidoglycan mediates lysostaphin binding to the cell wall envelope of Staphylococcus aureus. J Bacteriol 188:2463-2472.

64. Low LY, Yang C, Perego M, Osterman A, Liddington R. 2011. Role of net charge on catalytic domain and influence of cell wall binding domain on bactericidal activity, specificity, and host range of phage lysins. J Biol Chem 286:34391-34403.

65. Horgan M, O'Flynn G, Garry J, Cooney J, Coffey A, Fitzgerald GF, Ross RP, McAuliffe O. 2009. Phage lysin LysK can be truncated to its CHAP domain and retain lytic activity against live antibiotic-resistant staphylococci. Appl Environ Microbiol 75:872-874.

66. Morita M, Tanji Y, Mizoguchi K, Soejima A, Orito Y, Unno H. 2001. Antibacterial activity of *Bacillus amyloliquefaciens* phage endolysin without holin conjugation. J Biosci Bioeng 91:469-473.

67. Safari F, Sharifi M, Farajnia S, Akbari B, Ahmadi MKB, Negahdaripour M, Ghasemi Y. 2020. The interaction of phages and bacteria: the co-evolutionary arms race. Crit Rev Biotechnol 40:119-137.

68. Huang Y, Niu B, Gao Y, Fu L, Li W. 2010. CD-HIT Suite: a web server for clustering and comparing biological sequences. Bioinformatics 26:680-682.

69. Madeira F, Park Ym, Lee J, Buso N, Gur T, Madhusoodanan N, Basutkar P, Tivey ARN, Potter SC, Finn RD, Lopez R. 2019. The EMBL-EBI search and sequence analysis tools APIs in 2019. Nucleic Acids Res 47:W636-W641.

70. Potter SC, Luciani A, Eddy SR, Park Y, Lopez R, Finn RD. 2018. HMMER web server: 2018 update. Nucleic Acids Res 46:W200-W204.

71. Vázquez R, García E, García P. 2020. Curated phage lysins collection including identifiers, amino acid sequences, functional domain predictions, architectures and physicochemical properties calculations doi:http://dx.doi.org/10.20350/digitalCSIC/12674, Digital.CSIC.

72. Osorio D, Rondón-Villarreal P, Torres R. 2015. Peptides: a package for data mining of antimicrobial peptides. R Journal 7:4-14.
73. Dawson RMC. 1986. Data for biochemical research, 3rd ed. Clarendon Press, Oxford.
74. Kyte J, Doolittle RF. 1982. A simple method for displaying the hydropathic character of a protein. J Mol Biol 157:105-132.
75. Eisenberg D, Weiss RM, Terwilliger TC. 1984. The hydrophobic moment detects periodicity in protein hydrophobicity. Proc Natl Acad Sci USA 81:140-144.
76. Zallot R, Oberg N, Gerlt JA. 2019. The EFI Web Resource for Genomic Enzymology Tools: Leveraging Protein, Genome, and Metagenome Databases to Discover Novel Enzymes and Metabolic Pathways. Biochemistry 58:4169-4182.
77. Shannon P, Markiel A, Ozier O, Baliga NS, Wang JT, Ramage D, Amin N, Schwikowski B, Ideker T. 2003. Cytoscape: a software environment for integrated models of biomolecular interaction networks. Genome Res 13:2498-2504.
78. Wickham H. 2016. ggplot2 - Elegant Graphics for Data Analysis, 2nd ed doi:10.1007/978-3-319-24277-4. Springer International Publishing, Switzerland.
79. Wilcox RR. 2012. Introduction to Robust Estimation & Hypothesis Testing, 3rd ed. Elsevier Inc., Amsterdam.
80. Wilcox RR, Tian TS. 2011. Measuring effect size: a robust heteroscedastic approach for two or more groups. J Appl Stat 38:1359-1368.
81. Mair P, Wilcox R. 2020. Robust statistical methods in R using the WRS2 package. Behav Res Methods 52:464-488.

LEGENDS TO THE FIGURES

FIG 1 General properties of lysins from phages that infect G+ or G− bacteria. (A) Distribution of the number of PF hits predicted per protein. (B) Distribution of protein lengths. (C and D) Distributions of the number of aa before (C) or after (D) predicted EADs. (E) Distribution of domain types. (F) PF domains variability (different colours stand for different PF domain families, corresponding to those shown in Table 1). In distribution charts (B, C, D) Y-axis shows an estimation of the distribution density.

FIG 2 Differential distribution of PF hits among G− and G+ bacterial hosts. Y-axis shows the proportion of PF hits found in G+ within a given domain family. Grey bars and numbers above represent the total number of hits of each PF domain.

FIG 3 Heatmap of PF hits distribution across host bacterium genera. Numbers within each tile indicate the number of hits predicted for the corresponding taxon and PF family. The colour scale represents the number of hits from low (red) to high number

(yellow). Grey bars at the right represent the total number of PF hits predicted within each genus.

FIG 4 Relevant architectures observed in lysins from phages infecting different taxonomic groups of bacteria. Different colours mean different domains; brackets denote domains that appear only in some representatives of the depicted architecture.

FIG 5 Differential distribution of CWBDs and catalytic activities across peptidoglycan chemotypes and taxonomic groups of bacterial hosts. (A) Schematic representation of the relevant peptidoglycan chemotypes present for the bacterial hosts in our dataset. (B) Distribution of CWBD PF hits among chemotypes. (C) Distribution of catalytic activities of EAD PF hits among chemotypes and taxonomic groups.

FIG 6 Random forest prediction and classification of Gram group of bacterial host based of lysins physicochemical properties. (A) ROC curve of the random forest predictive model (TRP: true positive rate, FPR: false positive rate). ROC best point of positive group (G+) probability for outcome maximization is presented, as well as the AUC. (B) Random forest casting of bacterial host Gram group on the testing subset of lysin sequences. The dashed line represents the G+ probability threshold for classification based on the ROC best point. (C) Relative importance of each of the four descriptors used for classification within the model. (D) MDS plot of the training subset according to the proximity matrix derived from the random forest.

FIG 7 Differential physicochemical properties distribution among G+ and G− phage lysins. (A) Distribution of net properties calculated along the whole protein sequences of lysins from phages infecting G− or G+. (B) Local computation of physicochemical properties. Each dot represents the particular value calculated for an 11-aa window in a given lysin. Continuous lines are average tendencies based on either all G− or all G+

847 data points. (C) Distribution of different properties at quartiles of lysin sequences.
848 Asterisks indicate p-values (** ≤ 0.01, *** ≤ 0.001) obtained from the Yuen-Welch test
849 for trimmed means with a trimming level of γ = 0.2; ES indicates the Wilcox and Tian's
850 ζ measurement of effect size.

851 **FIG 8** Net charge distribution of lysins from G− infecting phages classified according
852 to the predicted EAD. Rightmost grey bars depict the number of lysins classified into
853 each EAD group (lysins within NA group are those for which an EAD was not
854 assigned). All groups were compared with the distribution of the *Amidase_2* domain, as
855 a highly represented, near-neutral control using Welch's test on γ = 0.2 trimmed means
856 with *post hoc* Bonferroni correction (*, *p*-value ≤ 0.05; **, *p*-value ≤ 0.01; ***, *p*-value
857 ≤ 0.001).

858 **TABLE 1.** Distribution of PF hits of phage lysins from Gram-positive and Gram-
859 negative bacteria[a]

860

Domain	Domain type	G+ (%)	G– (%)	Total	Encoded by phages of:
3D	EAD	7		7	
Amidase_2	EAD	547 (85.7)	91 (14.3)	638	Widely distributed in G+
Amidase_3	EAD	93 (81.6)	21 (1.4)	114	*Bacillus, Streptococcus, Clostridium, Staphylococcus*
Amidase_5	EAD	81 (100)		81	*Streptococcus, Lactococcus*
CHAP	EAD	186 (93.9)	12(6.1)	198	*Streptococcus, Staphylococcus, Streptomyces, Arthrobacter*
Cutinase	EAD	24		24	
FSH1	EAD	3		3	
Glucosaminidase	EAD	73 (97.3)	2 (2.7)	75	*Streptococcus*
Glyco_hydro_19	EAD	9 (14.3)	54 (85.7)	63	*Acinetobacter* and other genera
Glyco_hydro_25	EAD	142 (100)		142	*Lactobacillus, Bacillus, Streptococcus*
Glyco_hydro_108	EAD		43 (100)	43	Widely distributed in G–
GPW_gp25	EAD		12	12	
Hydrolase_2	EAD	3 (5.8)	49 (94.2)	52	*Escherichia, Pseudomonas, Vibrio*
Muramidase	EAD		35 (100)	35	*Pseudomonas, Burkholderia*
NLPC_P60	EAD	7	6	13	

PE-PPE	EAD	13		13	
Peptidase_C39_2	EAD	42 (100)		42	*Mycobacterium*
Peptidase_C93	EAD		4	4	
Peptidase_M15_3	EAD		10	10	
Peptidase_M15_4	EAD	96 (71.1)	39 (28.9)	135	*Mycobacterium, Bacillus*
Peptidase_M23	EAD	77 (97.5)	2 (2.5)	79	*Arthrobacter, Mycobacterium, Rhodococcus*
Pesticin	EAD		2	2	
Phage_lysozyme	EAD	32 (8.0)	366 (92.0)	398	Widely distributed in G–
Phage_lysozyme2	EAD	1		1	
Prok-JAB	EAD		1	1	
Prophage_tail	EAD	3		3	
SLT	EAD	6	16	22	
Transglycosylase	EAD	32 (100)		32	*Mycobacterium*
Amidase02_C	CWBD	20		20	
Big_2	CWBD	1		1	
CW_7	CWBD	125 (100)		125	*Streptococcus, Arthrobacter, Streptomyces*
CW_binding_1	CWBD (repeat)	205 (100)		205	*Streptococcus*
CW_binding_2	CWBD (repeat)	3		3	
DUF3597	CWBD	5		5	
LGFP	CWBD (repeat)	31 (100)		31	*Rhodococcus*
LysM	CWBD	210 (97.7)	5 (2.3)	215	Widely distributed in G+
PG_binding_1	CWBD	130 (83.3)	26 (16.7)	156	*Mycobacterium, Bacillus, Streptomyces*
PG_binding_3	CWBD		40 (100)	40	Widely distributed in G–
PSA_CBD	CWBD	13		13	
SH3_3	CWBD	20	1	21	
SH3_5	CWBD	164 (100)		164	*Streptococcus, Staphylococcus, Lactobacillus, Bacillus*
SPOR	CWBD	5		5	
ZoocinA_TRD	CWBD	50 (100)		50	*Streptococcus, Enterococcus*
Gp5_C	Structural		3	3	
Gp5_OB	Structural		3	3	

[a] Percentages and further remarks are only shown for domains represented by, at least, 30 hits

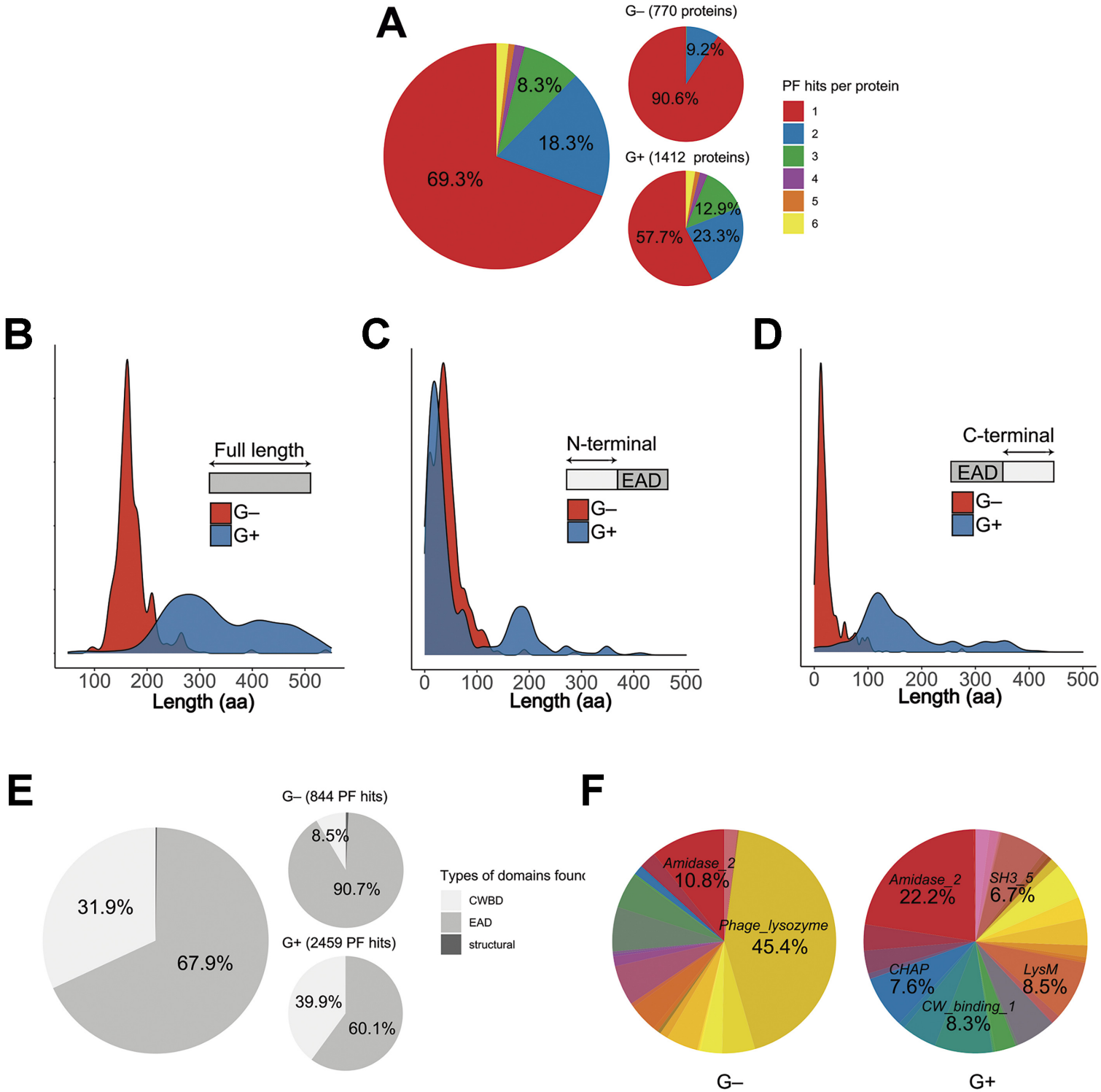
A
G– (770 proteins)
9.2%
90.6%
G+ (1412 proteins)
12.9%
57.7%
23.3%
8.3%
18.3%
69.3%
PF hits per protein
1
2
3
4
5
6
B
Full length
G–
G+
100 200 300 400 500
Length (aa)
C
N-terminal
EAD
G–
G+
0 100 200 300 400 500
Length (aa)
D
C-terminal
EAD
G–
G+
0 100 200 300 400 500
Length (aa)
E
G– (844 PF hits)
8.5%
90.7%
G+ (2459 PF hits)
39.9%
60.1%
31.9%
67.9%
Types of domains found
CWBD
EAD
structural
F
Amidase_2
10.8%
Phage_lysozyme
45.4%
G–
Amidase_2
22.2%
SH3_5
6.7%
CHAP
7.6%
LysM
8.5%
CW_binding_1
8.3%
G+

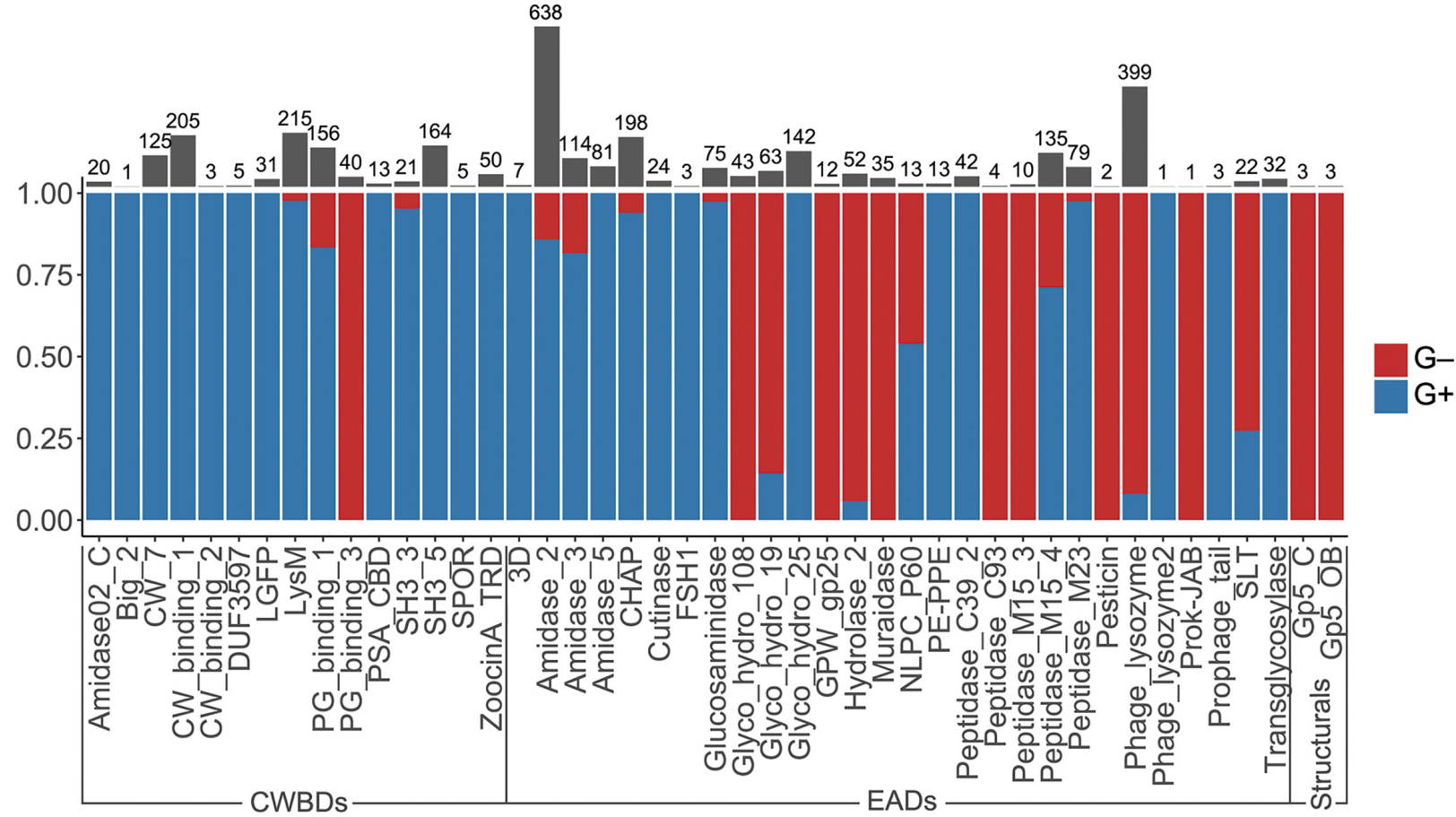
20
1
125
205
3
5
31
215
156
40
13
21
164
5
50
7
638
114
81
198
24
3
75
43
63
142
12
52
35
13
13
42
4
10
135
79
2
399
1
1
3
22
32
3
3
1.00
0.75
0.50
0.25
0.00
G–
G+
Amidase02_C
Big_2
CW_7
CW_binding_1
CW_binding_2
DUF3597
LGFP
LysM
PG_binding_1
PG_binding_3
PSA_CBD
SH3_3
SH3_5
SPOR
ZoocinA_TRD
3D
Amidase_2
Amidase_3
Amidase_5
CHAP
Cutinase
FSH1
Glucosaminidase
Glyco_hydro_108
Glyco_hydro_19
Glyco_hydro_25
GPW_gp25
Hydrolase_2
Muraidase
NLPC_P60
PE-PPE
Peptidase_C39_2
Peptidase_C93
Peptidase_M15_3
Peptidase_M15_4
Peptidase_M23
Pesticin
Phage_lysozyme
Phage_lysozyme2
Prok-JAB
Prophage_tail
SLT
Transglycosylase
Gp5_C
Gp5_OB
CWBDs
EADs
Structurals

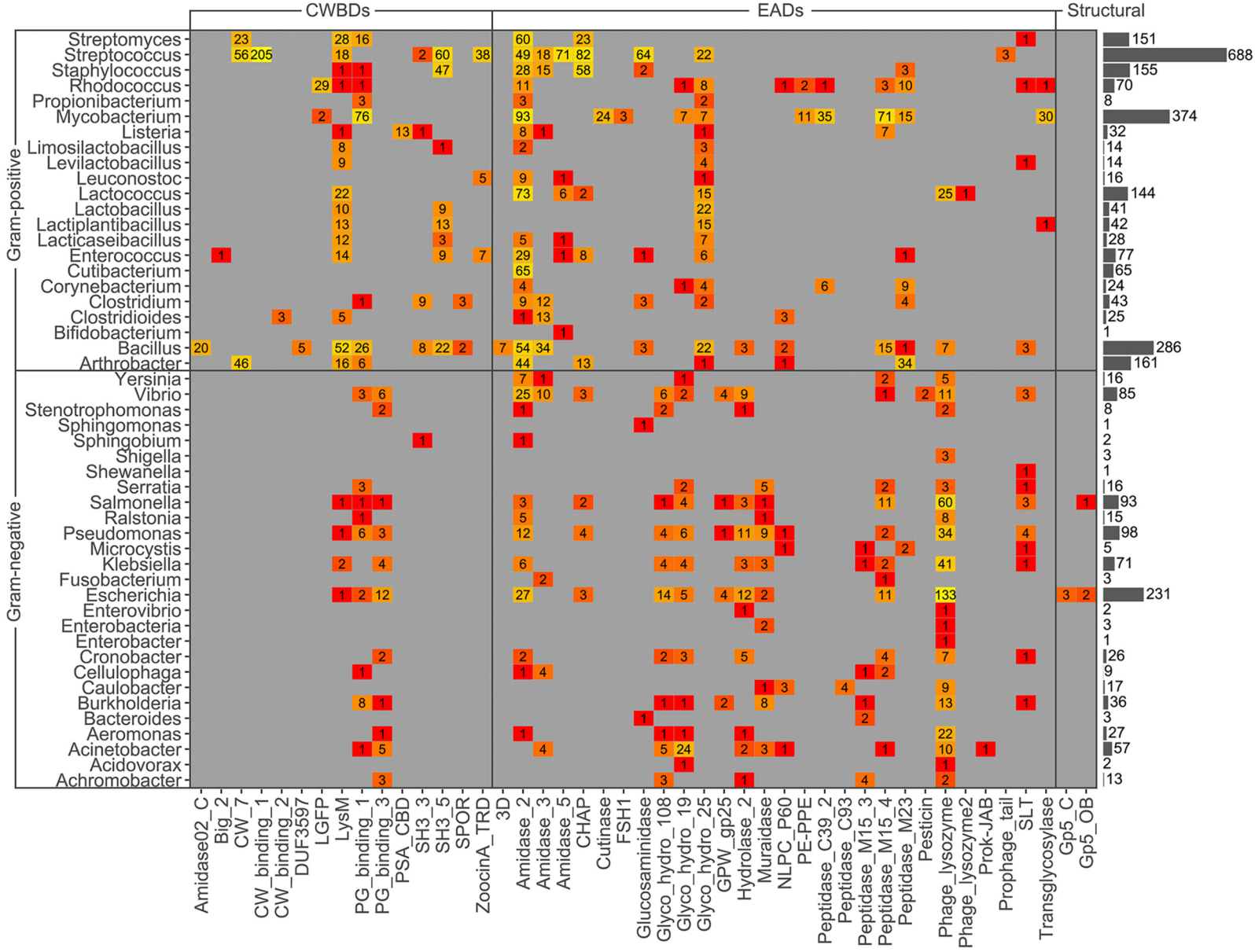
CWBDs
EADs
Structural
Gram-positive
Gram-negative
Streptomyces
Streptococcus
Staphylococcus
Rhodococcus
Propionibacterium
Mycobacterium
Listeria
Limosilactobacillus
Levilactobacillus
Leuconostoc
Lactococcus
Lactobacillus
Lactiplantibacillus
Lacticaseibacillus
Enterococcus
Cutibacterium
Corynebacterium
Clostridium
Clostridioides
Bifidobacterium
Bacillus
Arthrobacter
Yersinia
Vibrio
Stenotrophomonas
Sphingomonas
Sphingobium
Shigella
Shewanella
Serratia
Salmonella
Ralstonia
Pseudomonas
Microcystis
Klebsiella
Fusobacterium
Escherichia
Enterovibrio
Enterobacteria
Enterobacter
Cronobacter
Cellulophaga
Caulobacter
Burkholderia
Bacteroides
Aeromonas
Acinetobacter
Acidovorax
Achromobacter
151
688
155
70
8
374
32
14
14
16
144
41
42
28
77
65
24
43
25
1
286
161
16
85
8
1
2
3
1
16
93
15
98
5
71
3
231
2
3
1
26
9
17
36
3
27
57
2
13
Amidase02_C
Big_2
CW_7
CW_binding_1
CW_binding_2
DUF3597
LGFP
LysM
PG_binding_1
PG_binding_3
PSA_CBD
SH3_3
SH3_5
SPOR
ZoocinA_TRD
3D
Amidase_2
Amidase_3
Amidase_5
CHAP
Cutinase
FSH1
Glucosaminidase
Glyco_hydro_108
Glyco_hydro_19
Glyco_hydro_25
GPW_gp25
Hydrolase_2
Muraidase
NLPC_P60
PE-PPE
Peptidase_C39_2
Peptidase_C93
Peptidase_M15_3
Peptidase_M15_4
Peptidase_M23
Pesticin
Phage_lysozyme
Phage_lysozyme2
Prok-JAB
Prophage_tail
SLT
Transglycosylase
Gp5_C
Gp5_OB

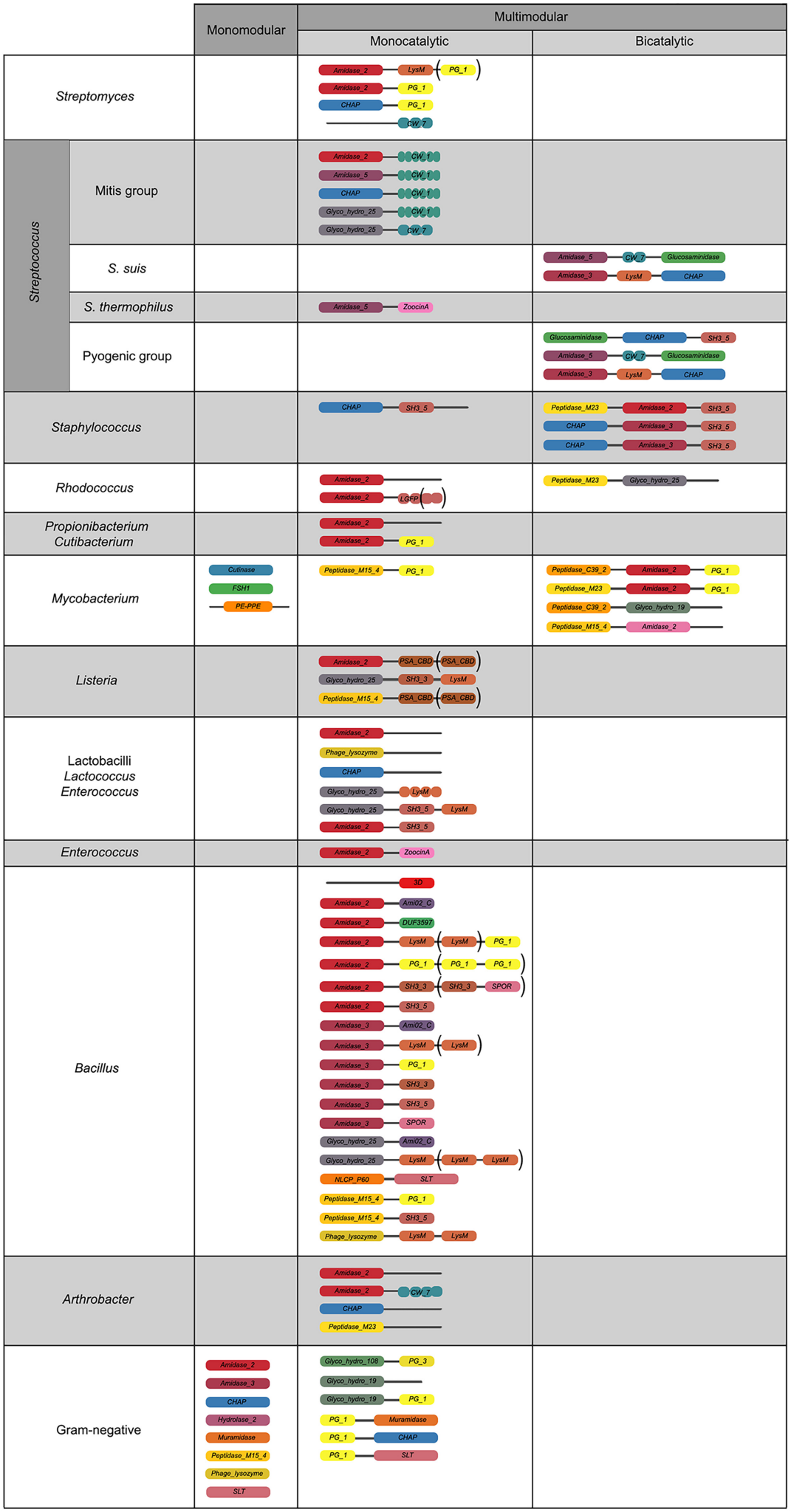
Monomodular
Multimodular
Monocatalytic
Bicatalytic
Streptomyces
Amidase_2 LysM PG_1
Amidase_2 PG_1
CHAP PG_1
CW_7
Streptococcus
Mitis group
Amidase_2 CW_1
Amidase_5 CW_1
CHAP CW_1
Glyco_hydro_25 CW_1
Glyco_hydro_25 CW_7
S. suis
Amidase_5 CW_7 Glucosaminidase
Amidase_3 LysM CHAP
S. thermophilus
Amidase_5 ZoocinA
Pyogenic group
Glucosaminidase CHAP SH3_5
Amidase_5 CW_7 Glucosaminidase
Amidase_3 LysM CHAP
Staphylococcus
CHAP SH3_5
Peptidase_M23 Amidase_2 SH3_5
CHAP Amidase_3 SH3_5
CHAP Amidase_3 SH3_5
Rhodococcus
Amidase_2
Amidase_2 LGFP
Peptidase_M23 Glyco_hydro_25
Propionibacterium
Cutibacterium
Amidase_2
Amidase_2 PG_1
Mycobacterium
Cutinase
FSH1
PE-PPE
Peptidase_M15_4 PG_1
Peptidase_C39_2 Amidase_2 PG_1
Peptidase_M23 Amidase_2 PG_1
Peptidase_C39_2 Glyco_hydro_19
Peptidase_M15_4 Amidase_2
Listeria
Amidase_2 PSA_CBD PSA_CBD
Glyco_hydro_25 SH3_3 LysM
Peptidase_M15_4 PSA_CBD PSA_CBD
Lactobacilli
Lactococcus
Enterococcus
Amidase_2
Phage_lysozyme
CHAP
Glyco_hydro_25 LysM
Glyco_hydro_25 SH3_5 LysM
Amidase_2 SH3_5
Enterococcus
Amidase_2 ZoocinA
Bacillus
3D
Amidase_2 Ami02_C
Amidase_2 DUF3597
Amidase_2 LysM LysM PG_1
Amidase_2 PG_1 PG_1 PG_1
Amidase_2 SH3_3 SH3_3 SPOR
Amidase_2 SH3_5
Amidase_3 Ami02_C
Amidase_3 LysM LysM
Amidase_3 PG_1
Amidase_3 SH3_3
Amidase_3 SH3_5
Amidase_3 SPOR
Glyco_hydro_25 Ami02_C
Glyco_hydro_25 LysM LysM LysM
NLCP_P60 SLT
Peptidase_M15_4 PG_1
Peptidase_M15_4 SH3_5
Phage_lysozyme LysM LysM
Arthrobacter
Amidase_2
Amidase_2 CW_7
CHAP
Peptidase_M23
Gram-negative
Amidase_2
Amidase_3
CHAP
Hydrolase_2
Muramidase
Peptidase_M15_4
Phage_lysozyme
SLT
Glyco_hydro_108 PG_3
Glyco_hydro_19
Glyco_hydro_19 PG_1
PG_1 Muramidase
PG_1 CHAP
PG_1 SLT

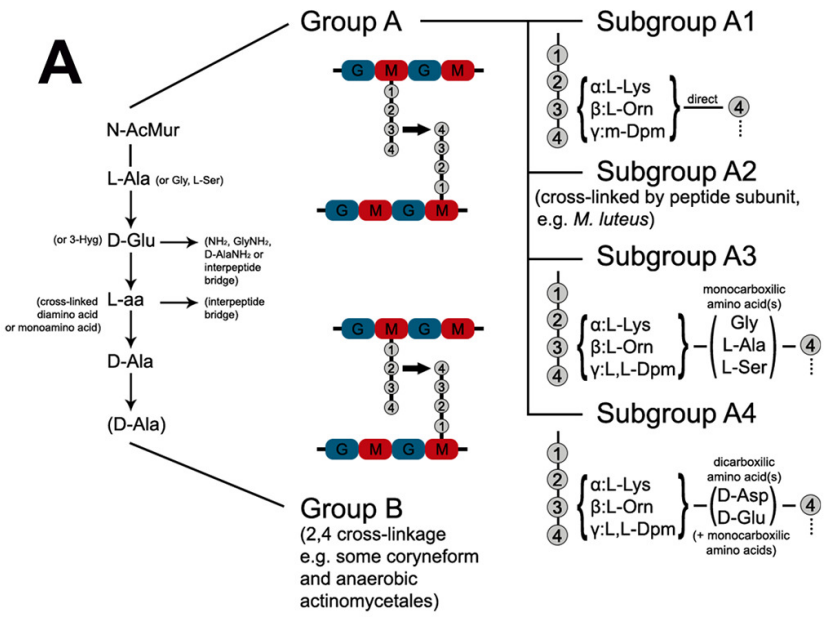
A
Group A
N-AcMur
L-Ala (or Gly, L-Ser)
(or 3-Hyg) D-Glu
(NH2, GlyNH2, D-AlaNH2 or interpeptide bridge)
(cross-linked diamino acid or monoamino acid)
L-aa
(interpeptide bridge)
D-Ala
(D-Ala)
Group B
(2,4 cross-linkage
e.g. some coryneform
and anaerobic
actinomycetales)
Subgroup A1
α:L-Lys
β:L-Orn
γ:m-Dpm
direct
Subgroup A2
(cross-linked by peptide subunit,
e.g. M. luteus)
Subgroup A3
α:L-Lys
β:L-Orn
γ:L,L-Dpm
monocarboxilic amino acid(s)
Gly
L-Ala
L-Ser
Subgroup A4
α:L-Lys
β:L-Orn
γ:L,L-Dpm
dicarboxilic amino acid(s)
D-Asp
D-Glu
(+ monocarboxilic amino acids)

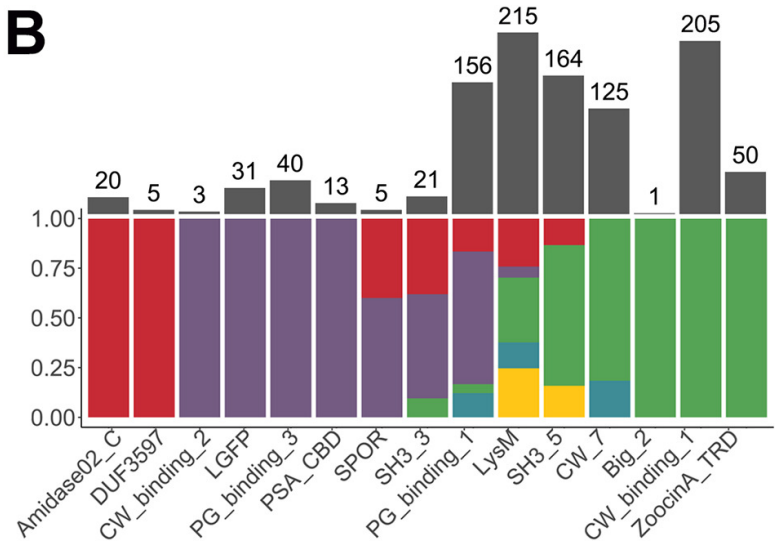
B
20
5
3
31
40
13
5
21
156
215
164
125
1
205
50
1.00
0.75
0.50
0.25
0.00
Amidase02_C
DUF3597
CW_binding_2
LGFP
PG_binding_3
PSA_CBD
SPOR
SH3_3
PG_binding_1
LysM
SH3_5
CW_7
Big_2
CW_binding_1
ZoocinA_TRD

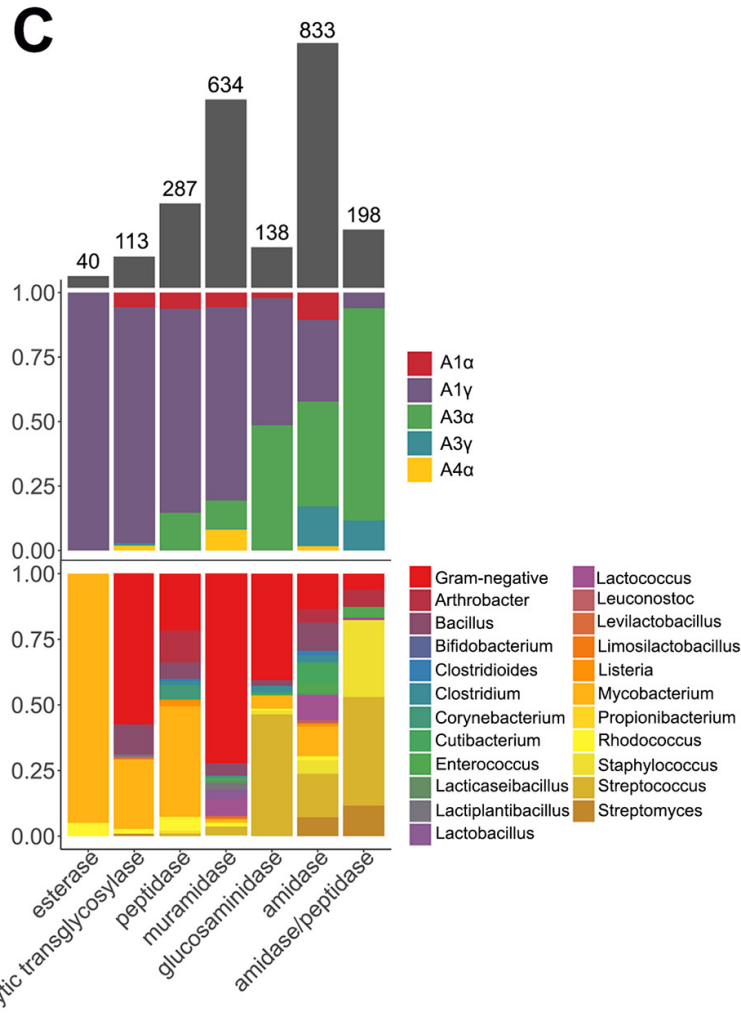
C
40
113
287
634
138
833
198
1.00
0.75
0.50
0.25
0.00
A1α
A1γ
A3α
A3γ
A4α
Gram-negative
Arthrobacter
Bacillus
Bifidobacterium
Clostridioides
Clostridium
Corynebacterium
Cutibacterium
Enterococcus
Lacticaseibacillus
Lactiplantibacillus
Lactobacillus
Lactococcus
Leuconostoc
Levilactobacillus
Limosilactobacillus
Listeria
Mycobacterium
Propionibacterium
Rhodococcus
Staphylococcus
Streptococcus
Streptomyces
esterase
lytic transglycosylase
peptidase
muramidase
glucosaminidase
amidase
amidase/peptidase

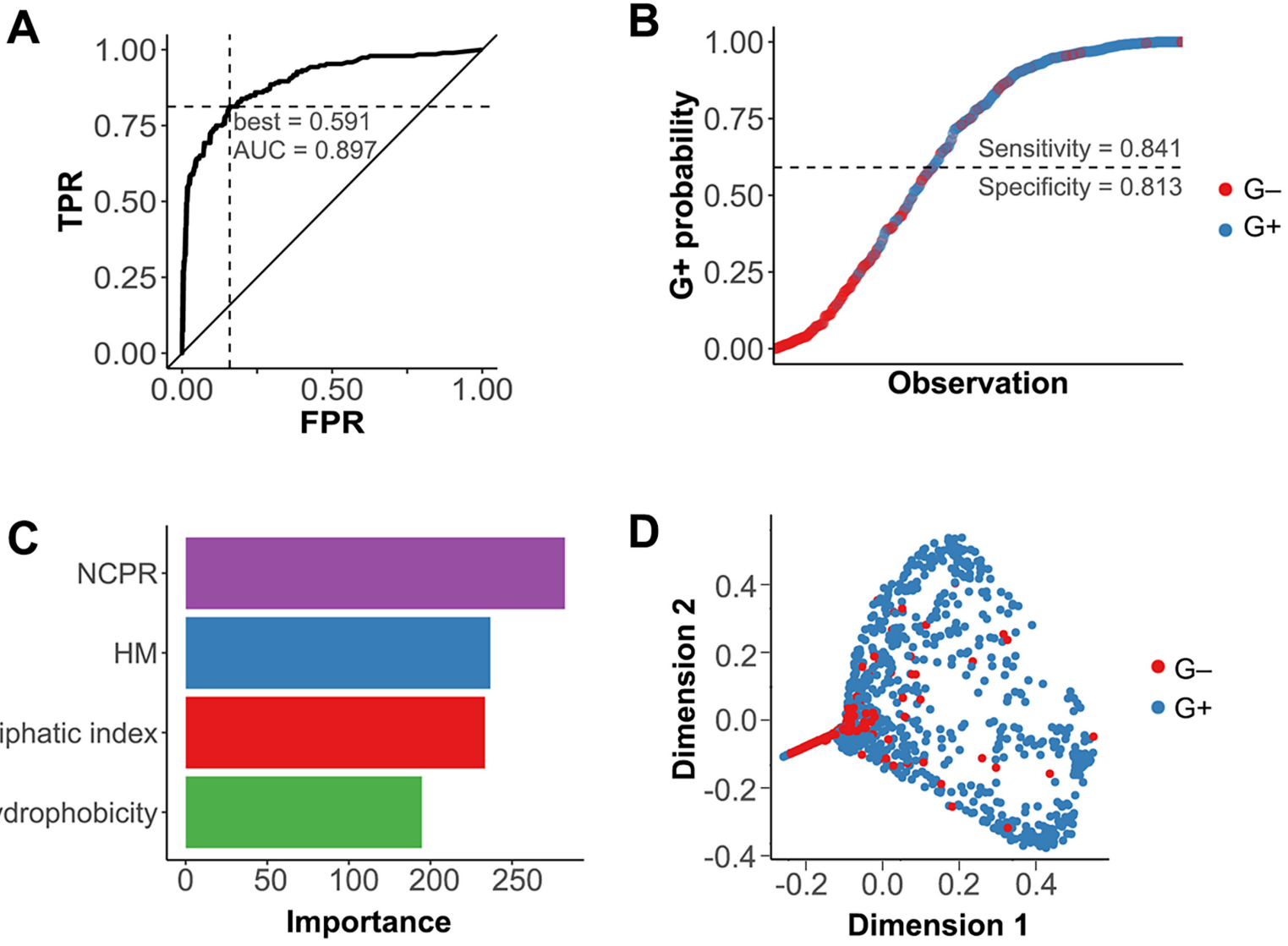
A
1.00
0.75
0.50
0.25
0.00
TPR
best = 0.591
AUC = 0.897
0.00
0.50
1.00
FPR
B
1.00
0.75
0.50
0.25
0.00
G+ probability
Sensitivity = 0.841
Specificity = 0.813
G–
G+
Observation
C
NCPR
HM
Aliphatic index
Hydrophobicity
0
50
100
200
250
Importance
D
0.4
0.2
0.0
-0.2
-0.4
Dimension 2
G–
G+
-0.2
0.0
0.2
0.4
Dimension 1

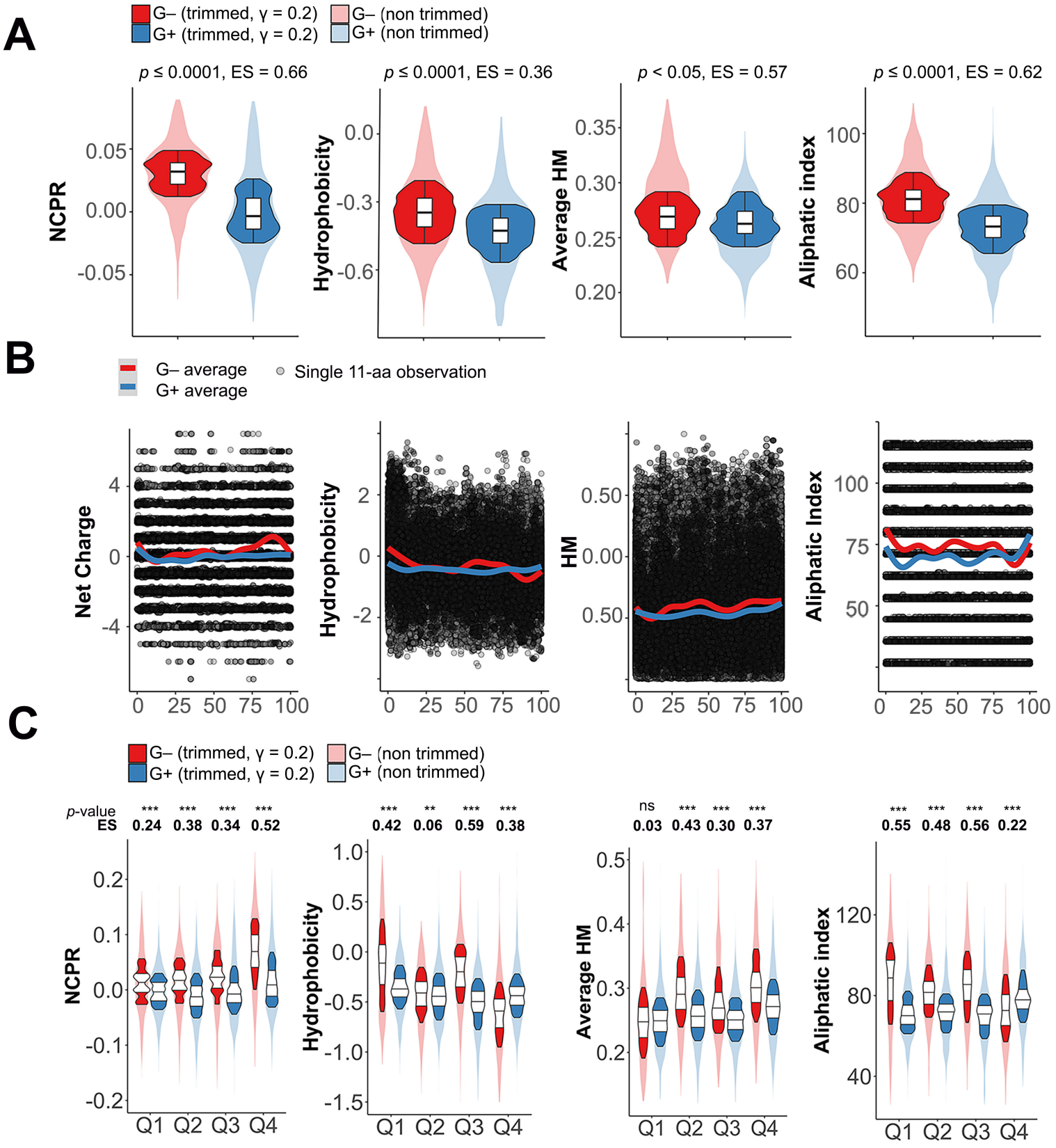
A
G– (trimmed, γ = 0.2)
G+ (trimmed, γ = 0.2)
G– (non trimmed)
G+ (non trimmed)
p ≤ 0.0001, ES = 0.66
p ≤ 0.0001, ES = 0.36
p < 0.05, ES = 0.57
p ≤ 0.0001, ES = 0.62
NCPR
Hydrophobicity
Average HM
Aliphatic index
B
G– average
G+ average
Single 11-aa observation
Net Charge
Hydrophobicity
HM
Aliphatic Index
C
G– (trimmed, γ = 0.2)
G+ (trimmed, γ = 0.2)
G– (non trimmed)
G+ (non trimmed)
p-value
ES
*** *** *** ***
0.24 0.38 0.34 0.52
*** ** *** ***
0.42 0.06 0.59 0.38
ns *** *** ***
0.03 0.43 0.30 0.37
*** *** *** ***
0.55 0.48 0.56 0.22
NCPR
Hydrophobicity
Average HM
Aliphatic index
Q1 Q2 Q3 Q4

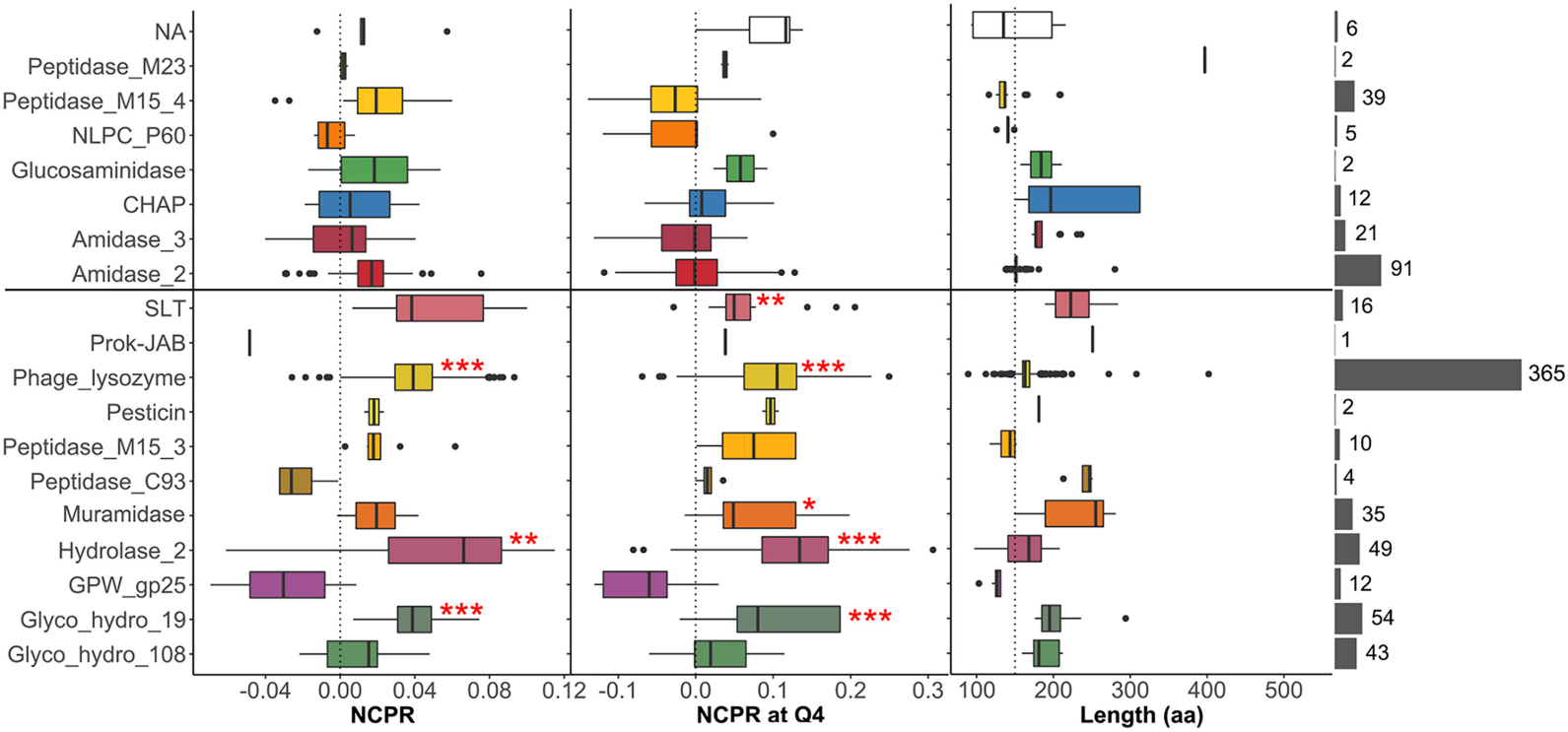
NA
Peptidase_M23
Peptidase_M15_4
NLPC_P60
Glucosaminidase
CHAP
Amidase_3
Amidase_2
SLT
Prok-JAB
Phage_lysozyme
Pesticin
Peptidase_M15_3
Peptidase_C93
Muramidase
Hydrolase_2
GPW_gp25
Glyco_hydro_19
Glyco_hydro_108
6
2
39
5
2
12
21
91
16
1
365
2
10
4
35
49
12
54
43
-0.04
0.00
0.04
0.08
0.12
NCPR
-0.1
0.0
0.1
0.2
0.3
NCPR at Q4
100
200
300
400
500
Length (aa)